FIBER COMPOSITE ELEMENTS AND TECHNIQUES AS NON-METALLIC REINFORCEMENT OF CONCRETE

BRITE PROJECT 4142 / BREU - CT 91 0515

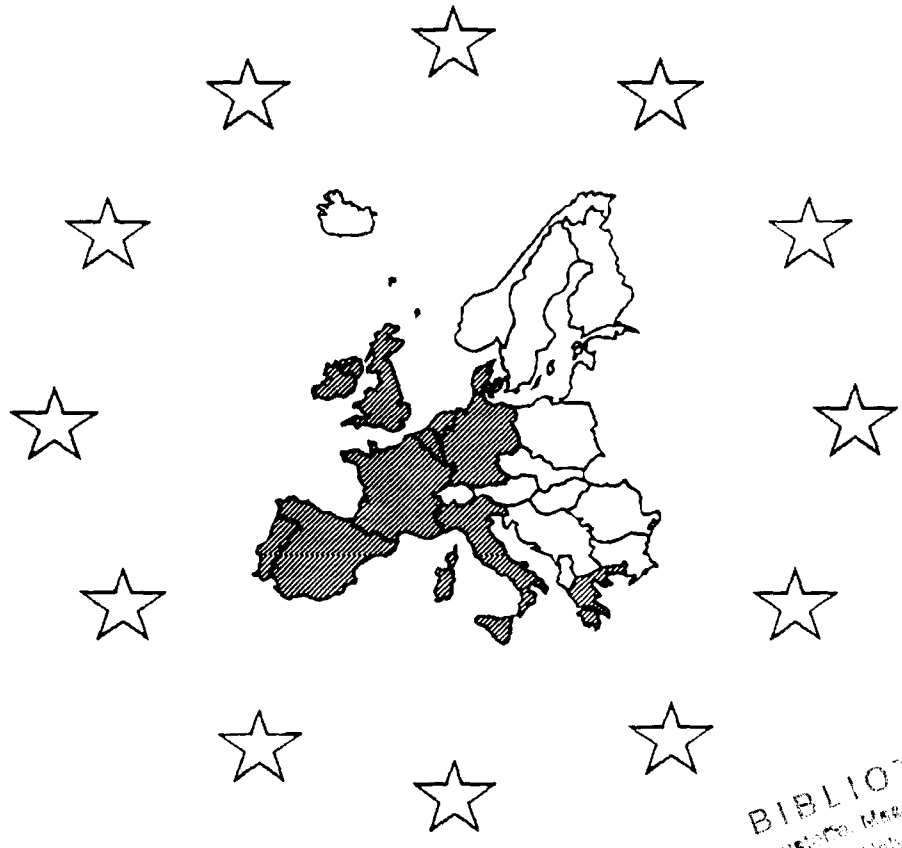

Test methods for the assessment of mechanical properties of FRP

F.S. Rostásy, C. Hankers, M. Scheibe

Report No.: BREU 1-93

SICOM AKZO HBG iBMB/TU Braunschweig Magnel Laboratory Gent

March 1993

NOTATION

(in accordance to EC2. pt.1)

1. UNITS

For calculations, the following units are recommended:

- forces and loads : kN, kN/m, kN/m^2
- unit mass : kg/m^3
- unit weight : kN/m^3
- stresses and strengths : N/mm^2 (= MPa; = MN/m^2)
- moments (bending...) : kNm
- strain : °/••

2. LATIN UPPER CASE SYMBOLS

2.1. GEOMETRY

A	Area (in general)
A_b	Total cross sectional area of a concrete section
$A_{b,eff}$	Effective tensile zone of reinforcement
A_{bt}	Tensile zone in the uncracked state of concrete
A_c	Total cross sectional area of a composite element
A_f	Total cross sectional area of fibers
A_m	Total cross sectional area of resin matrix
A_p	Area of a prestressing steel unit
A_s	Area of reinforcement within the tensile zone
$A_{s,min}$	Minimum area of longitudinal tensile reinforcement
A_{s1}	Area of tension reinforcement effective at the section
A_{s2}	Area of compressive reinforcement
$A_{s,prov}$	Area of steel provided
$A_{s,req}$	Area of steel required
$A_{s,surf}$	Area of surface reinforcement
A_{st}	Area of a transverse bar
A_{sv}	Additional transverse steel perpendicular to the lower face
I_b	Second moment of area of a concrete section
R	Curvature radius of tendon
T	Torsional moment
W_b	Section modulus of concrete
W_t	Torsional resistance moment

2.2 ACTIONS, RESISTANCES, FORCES AND MOMENTS

A	Accidental action
G	Permanent action
P	Prestressing force
Q	Variable action
S	Characteristic action
S_d	Design action
R	Resistance
R_d	Design resistance
R_k	Characteristic resistance
F	Force (in general)
F_c	Short-term tensile force of total composite cross-section
F_f	Short-term tensile force of total fiber cross-section
F_p	Short-term tensile force of prestressing steel
F_s	Short-term tensile force of reinforcing steel
F_{ck}	Characteristic short-term tensile breaking force of the composite
F_{fk}	Characteristic short-term tensile breaking force of total fiber cross-section
F_{pk}	Characteristic short-term breaking force of prestressing steel unit
F_{sk}	Characteristic short-term tensile breaking force of reinforcing steel
F_{cl}	Long-term force of total composite cross-section
F_{fl}	Long-term tensile breaking force of total fiber cross-section
F_{clk}	Characteristic long-term static breaking force of the composite element
F_{flk}	Characteristic long-term tensile force of total fiber cross-section
F_{cli}	Long-term force on force level α_i
F_{cm}	Mean short-term tensile breaking force of the investigated lot of FRP-elements
F_{cr}	Failure load after long-term loading of the composite
M	Bending moment (in general)
M_{cr}	Moment causing cracking
M_{Sd}	Design value of the applied internal bending moment
M_u	Ultimate bending moment
N_{Sd}	Design axial force (tension or compression)

N_u; N_{ud}	Design ultimate capacity of the section subjected to axial load only
P_d	Design value of the prestressing force at the ultimate limit state
$P_{k,inf}$; $P_{k,sup}$	Lower and upper characteristic value of the prestressing force for serviceability calculations
P_o	Initial force at the active end of the tendon immediately after stressing
$P_{o,max}$	Maximum permissible value of P_o
$P_{m,o}$	Mean value of the prestressing force immediately after stressing (post-tensioning) or transfer (pre-tensioning) at any point distance along the member (i.e. the force after immediate losses have occured)
$P_{m,t}$	Mean value of the prestressing force at time t, at any point distance x along the member
$P_{m,\infty}$	Mean value of the prestressing force, after all losses have occured, at any point distance x along the member
V_u	Ultimate shear capacity
ΔP	Loss of prestress
ΔP_c	Loss of prestress due to elastic deformation of the member at transfer
ΔP_{sl}	Loss of prestress due the anchorage slip
$\Delta P_\mu(x)$	Loss of prestress due to friction
$\Delta P_c(t)$	Loss of prestress due to creep, shrinkage and relaxation at time t

2.3 MATERIALS

E_b	Modulus of elasticity of normal weight concrete
E_{bd}	Design value of the secant modulus of elasticity
E_{bm}	Secant modulus of elasticity of normal weight concrete
$E_b(t)$	Tangent modulus of elasticity of normal weight concrete at time t
$E_{b(28)}$	Tangent modulus of elasticity of normal weight concrete at 28 days
$E_{bc,eff}$	Effective modulus of elasticity of normal weight concrete
E_{Lc};$E_{Lb,m}$	Secant modulus of elasticity of lightweight concrete
E_c	Modulus of elasticity of composite
E_f	Modulus of elasticity of fiber
E_m	Modulus of elasticity of matrix
E_s	Modulus of elasticity of reinforcement or prestressing steel

3. LATIN LOWER CASE LETTERS

3.1 GEOMETRY

b	Overall width of a cross-section, or actual flange width in a T or L beam
b_{eff}	Effective flange width of a T or L beam
b_z	Width of the tensile cross section
b_w	Width of the web on t, I or L beams
$b_{w,nom}$	Effective width of the web
c	Concrete cover
$\min c$	Minimum concrete cover
d	Effective depth of a cross-section
$\varnothing_n$	Diameter of a prestressing duct
d_g	Largest nominal maximum aggregate size
d_c	Diameter of a composite bar,etc.
d_f	Diameter of an individual fiber
d_s	Diameter of a reinforcing or prestressing bar
e	Eccentricity
f	Deflection
$f_{c,s}$	Increase of deflection due to creep and shrinkage
f_{tot}	Total deflection
h	Overall depth of a cross-section
h_f	Overall depth of a flange in T or L beams
k	Unintentional angular displacement of the tendons
l	Length, span (in general)
l_b	Basic anchorage length for reinforcement
l_{ba}	Anchorage length over which the tendon force in pretensioned members is fully transmitted to the concrete
l_{bp}	Transmission lenghth over which the prestressing force is fully transmitted to the concrete
l_c	Free length between anchorages
l_e	Gage length for the measurement of the axial strain
l_{eff}	Effective span of a beam
l_n	Clear distance between the faces of the supports
l_o	Length of span(s) between points of zero moment
$l_{p,eff}$	Dispersion length, over which the concrete stresses gradually disperse to a linear distribution across the section (effective transfer)
s	Spacing of the stirrups
s_v, s_h	Minimal vertical or horizonal distance of tendons

u	Perimeter of concrete cross section, having area A_b
v_f	Fiber volume in a composite cross section
v_m	Matrix volume in a composite cross section
w_k	Design crack width
x, y, z	Coordinates
z	Lever arm of internal forces
z_{cp}	Distance between the centre of gavity of the concrete section and the tendons

3.2 MATERIALS

f	strength (in general)
f_b	Compressive strength of concrete
$f_{bk,cube}$	Characteristic compressive cube strength of concrete at 28 days
f_{bm}	Mean value of concrete cylinder compressive strength
f_{btk}	Characteristic axial tensile strength of concrete
f_{btm}	Mean value of axial tensile strength of concrete
$f_{btk,0.05}$	Lower characteristic tensile strenth (5% fractile)
$f_{btk,0.95}$	Upper characteristic tensile strength (95% fractile)
$f_{bt,ax}$	Axial tensile strength of concrete
$f_{bt,fl}$	Flexural tensile strength of concrete
$f_{bt,sp}$	Splitting tensile strength of concrete
f_c	Tensile strength of composite
f_{ck}	Characteristic tensile strength of composite
$f_{c\tau i}$	interlaminar shear strength of a composite
$f_{c\tau s}$	surface strength of a composite
f_τ	bond strength between composite and concrete
f_f	Tensile strength of fiber of a composite
f_{fk}	Characteristic short-term tensile strength of fiber
f_m	Tensile strength of matrix of a composite
f_{mk}	Characteristic strength of matrix of a composite
f_p	Tensile strength of prestressing steel
f_{pk}	Characteristic tensile strength of prestressing steel
$f_{p0.1}$	0.1% proof-stress of prestressing steel
$f_{p0.1k}$	Characteristic 0.1% proof-stress of prestressing steel
f_t	Tensile strength of reinforcement
f_{tk}	Characteristic tensile strength of reinforcement
f_y	Yield stress of reinforcement

f_{yd} Design yield strength of reinforcement

f_{yk} Characteristic yield stress of reinforcement

f_{ywd} Design yield strength of stirrups

4. GREEK LOWER CASE LETTERS

4.1 GEOMETRY

α Inclination of shear reinforcement to the member axis

α Angle, ratio

β Spread angle of the prestressing force

μ Ratio (A_s/A_b)

μ Coefficient of friction between the tendons and their ducts

4.2 STRAIN AND STRESS

α_i Force level (F_{cli}/Z_{cm})

ϵ Strain (in general)

ϵ_u Ultimate strain

ϵ_b Compressive strain in the concrete

ϵ_{bu} Ultimate compressive strain in the concrete

ϵ_{bs} Basic shrinkage strain for normal weight concrete

$\epsilon_{bs\infty}$ Final shrinkage strain for normal weight concrete

ϵ_u Elongation of reinforcement or prestressing steel at maximum load

ϵ_c Elongation of composite at maximum load

ϵ_{cc} Creep strain

ϵ_f Elongation of fiber at maximum load

ϵ_m Elongation of matrix at maximum load

ϵ_p Elongation of prestressing steel at maximum load

ϵ_t Elongation of reinforcing steel at maximum load

$\Delta\epsilon_c$ Variation of elongation in the composite

$\Delta\epsilon_p$ Variation of elongation in the prestressing steel

σ Stress (in general)

$\sigma(t_0);\sigma(t)$ Stress at time t_0 or t

σ_b Stress in concrete

σ_{bg} Stress in the concrete adjacent to the tendons, due to self-weight and any other permanent actions

σ_{bp0} Initial stress in the concrete adjacent to the tendons, due to prestress

σ_{bS}	Compressive stress in the centre of gravity of a concrete cross section
σ_{bt}	Tensile stress in concrete
σ_c	Stress in a fiber composite
σ_f	Stress in an individual fiber of a composite
σ_m	Stress in matrix
σ_p	Stress in prestressing steel
$\sigma_m;\sigma_u;\sigma_o$	Middle-, lower- and upper stress under dynamic action
$\Delta\sigma_{pr}$	Variation of stress in the tendons at section x due to relaxation
$\Delta\sigma_{p,c+s+r}$	Variation of stress in the tendons due to creep, shrinkage and relaxation
τ	Shear stress
$\Delta\sigma$	Stress variation between lower and upper stress
$\Delta\sigma_{rel}$	Variation of stress of a composite due to relaxation

4.3 MATERIAL

α	Ratio (E_s/E_b or E_c/E_b)
α	Coefficient of linear thermal expansion (in general)
$\alpha_{T,b}$	Coefficient of linear thermal expansion of concrete
$\alpha_{T,c}$	Coefficient of linear thermal expansion of a fiber composite
$\alpha_{T,s}$	Coefficient of linear thermal expansion of reinforcing or prestressing steel
α_{cl}	Coefficient of linear thermal expansion of composite (longitudinal)
α_{ct}	Coefficient of linear thermal expansion of composite (transversal)
α_{fl}	Coefficient of linear thermal expansion of fiber (longitudinal)
α_{ft}	Coefficient of linear thermal expansion of fiber (transversal)
α_m	Coefficient of linear thermal expansion of matrix
ρ	Density
ρ_b	Density of concrete
ρ_c	Density of the composite element
ρ_f	Density of fibers
ρ_m	Density of matrix
μ_b	Poisson's ratio of concrete
μ_c	Poisson's ratio of composite
ϕ	Creep function
ψ	Relaxation function

4.4 SAFETY

γ_A	Partical safety factors for accidental actions A
γ_B	Partial safety factors for concrete material properties
γ_F	Partial safety factors for actions, F
γ_G	Partial safety factors for permanent actions G
γ_M	Partial safety factor for material property, taking account of uncertainties in the material properties itself and in the design model used
γ_P	Partial safety factors for actions associated with prestressing, P
γ_Q	Partial safety factors for variable actions Q
γ_S	Partial safety factor for the properties of reinforcement and prestressing steel
γ_f	Partial safety factor for actions without taking account of model uncertainties
γ_g	Partial safety factor for permanent actions without taking account of model undertainties
γ_m	Partial safety factor for a material property, taking account only of uncertainties in the material property

5. OTHER SYMBOLS

N	Number of load cycles
N_u	Number of load cycles until fracture
T	Temperature
ΔT	Temperature difference
n	Total number of wires and strands in a tendon
t	Time being considered
t_o	Time at initial loading of concrete
t_u	Time under load until fracture
t_{ui}	Time under force F_{cli} until fracture
μ	Mean value
σ	Standard deviation
v	Coefficient of variation

1. AIM OF REPORT

In the technical report [1] on task 1 "Evaluation of the potentials and production technologies of FRP" a state-of-the-art of the mechanical properties was - beyond other items - presented. It was shown that the determination of the mechanical properties of FRP requires suitable experimental techniques and subsequent test regulations. The existing standards dealing with the testing of FRP mostly pertain to laminated FRP. They are in many respects not suitable for the testing of FRP tensile elements in the shape of rods, strips or strands to be used for structural engineering applications.

If the results of tests performed at different laboratories are to be compared, the applied test methods must a least be known. For partners perseuing the same goal this requirement does not suffice. In this case, the comparability of test results requires that identical types of tests are also performed identically to preclude test-induced differences and falsifications. It is the aim of the report to present descriptions of the testing and measuring devices and prescriptions for the test procedures and also to set up an internal test standardization.

2. EXPERIMENTAL DETERMINATION OF THE MECHANICAL SHORT-TERM PROPERTIES

2.1 Axial Short-term Tensile Strength

2.1.1 Introductory remarks

The FRP elements used for structural concrete applications are unidirectional fiber composites in the shape of round bars and strands. They will in practical use to be axially stressed in tension, i.e. in parallelity to the fibers. Hence, the axial tensile strength under short-term and also under long-term force is one of the most important property.

In consequence of this fact, the testing of the axial tensile short-term strength is pre-eminently important. Not only for the structural use of the FRP element but also for the quality control of the production and for many

other aspects, the short-term tensile strength is the decisive reference property of the FRP element.

In spite of the importance of this value the state of test regulations is rather confusing and non-uniform. The test methods for high-strength composites generally follow the ASTM standards D 3039 and 23243 [2]. The German standard DIN 53 455 [3] refers to the ISO/DIS 527 "Plastics-Determination of Tensile Properties" [4]. The latter is identical with EN 61 "Fiber reinforced plastics, tensile properties" [5].

In all of these standards, the important fact that the FRP element has to be tested in its as-produced state is not fully considered. In view of these facts, the test reports as found in the literature only partly adhere to these standards. Mostly, product-specific test regulations and procedures were chosen which often differ from each other and which consequently aggravate the objective comparison between products.

2.1.2 On the difficulty to define the composite tensile strength

When testing the tensile strength of a prestressing steel wire of small diameter d_s and with a defined free length $l > 10$ to 20 d_s, the break of wire in the free length of specimen can usually be achieved. There is a lot of experimental experience available to ensure such desired failure mode. In such cases we obtain a true though volume-related strength value.

However, testing becomes more difficult for seven-wire and for multi-wire strands, especially if the strands are being compacted. This difficulty arises from two facts: the force introduction effect and the compound action effect. For large diameter bars, the introduction of the force in such a way to ensure break in free length causes great problems. We can conclude that also for prestressing steel the experimental derivation of the tensile strength of the material may be tarnished by falsifying effects.

The experimental determination of the tensile strength of an FRP element is also aggravated by the afore-mentioned effects. In addition, the pronounced strength anisotropy causes problems when anchoring the FRP element in the test machine.

It is not just a matter of scientific curiosity to know more about the true axial strength of an FRP element. Presupposing that such property exists and that it can be reliably tested or forecast, it has an important economic meaning, because it represents the highest level of structural utilization (FRP are expensive materials). A common but crude method to forecast the axial tensile strength is the rule of mixtures [6] in the form of

$$f_c \approx v_f \cdot f_f \tag{2.1}$$

in which the contribution of the matrix to the axial tensile strength f_c of the composite is entirely neglected. Equ.(2.1) assumes, s. Fig. 2.1, that

$$\sigma_m (1-v_f) << v_f f_f, \tag{2.2}$$

which justifies the omission of the contribution of the matrix, especially if the fiber volume is in the practical range of 50 to 70 Vol.-% and if polyesther and epoxy matrices are used. Certainly, the failure strain of the matrix ε_{mu} must exceed that of the fiber, a condition which is usually met.

The fiber strength f_f is a value usually given by the fiber producer. It must be regarded as a nominal breaking strength. It is derived on basis of tensile tests on bundles of variable numbers of resin-impregnated fibers in order to simulate the composite action within an FRP element with e.g. 50000 to 400000 individual fibers. Suitable practical procedures are applied. By such a procedure the reduction of the variability of the fiber strength and of the effect of the fiber length on its strength by composite interaction between fiber and matrix can be taken into account [6].

From [6] we conclude that the value f_f is not the tensile strength of the naked fiber of a certain length but represents its tensile strength in the embedded state. Then we may write for the theoretical mean tensile breaking force of the element

$$\text{cal } F_{cm} \approx A_c \cdot v_f \cdot f_f \tag{2.3}$$

if the value f_f is made known by the fiber producer.

It should be pointed out that the forecast with Eq.(2.3) will be a rather crude one. Even if the cross-section is known, it cannot be considered to

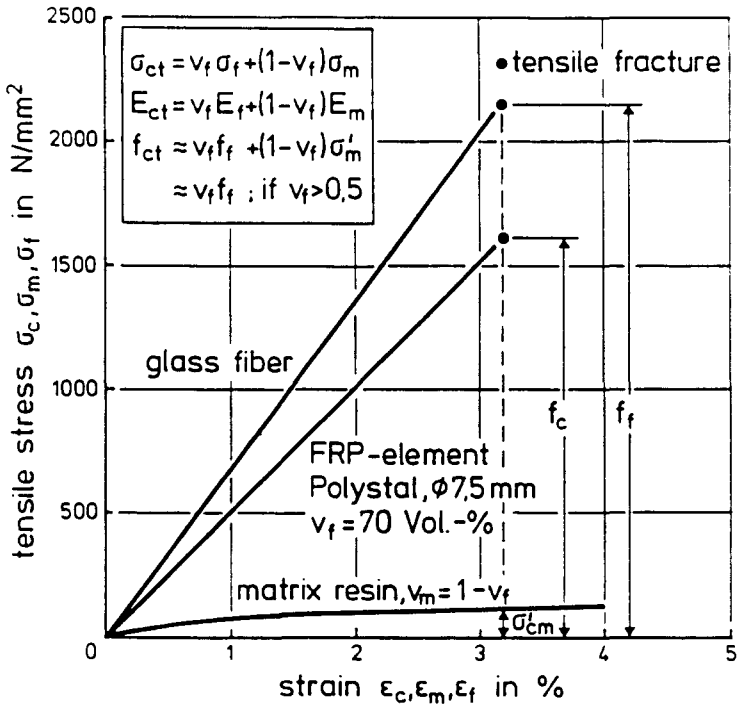

Fig. 2.1: Stress-Strain Lines of Components and Rule of Mixtures

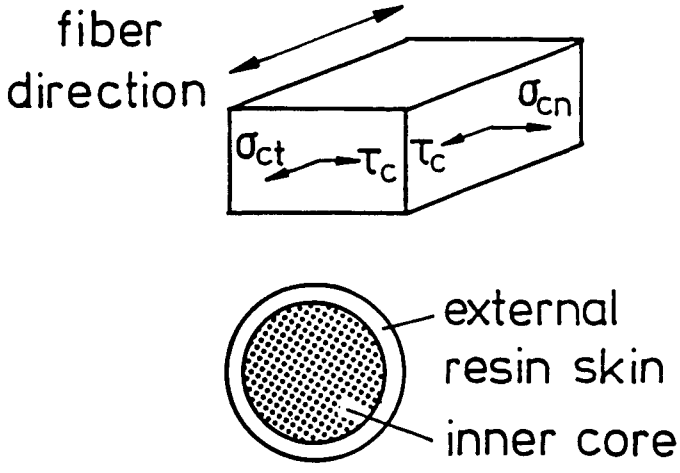

Fig. 2.2: Distribution of Components inside the Cross-Section

be uniformly interspersed with fibers. As shown by Fig. 2.2, there exists an outer region of resin without fibers.

These remarks show that the prediction of the tensile breaking strength is connected with several uncertainties. Extensive testing becomes inevitable.

2.1.3 Parameters of the axial tensile strength testing

The following parameters influence the axial tensile strength of an FRP element:

a.) cross-section A_c as well as the volume ratios v_f and v_m of fibers and the matrix;

b.) thickness of external layer of resin on the core of the element;

c.) mechanical properties of the components, inter- and intralaminar shear strength, shear strength between external layer and core;

d.) alignment of fibers and uniformity of fiber distribution, etc.

The parameters a.) to d.) pertain to the FRP element in its as-produced state. They all exhibit scatter. Besides these material parameters, the following ones are related to testing:

e.) loading or strain rate;

f.) free length of specimen;

g.) moisture content and temperature of element (pre-conditioning);

h.) type of anchorage

The influence of the material parameters on the tensile strength has been dealt with in [1]. The influence of the parameters of testing will be discussed in the sequel.

2.1.4 Influence of loading rate

The influence of the loading rate on the tensile strength of GFRP Polystal bars is discussed in detail in [7]. In Fig. 2.3 test results are presented.

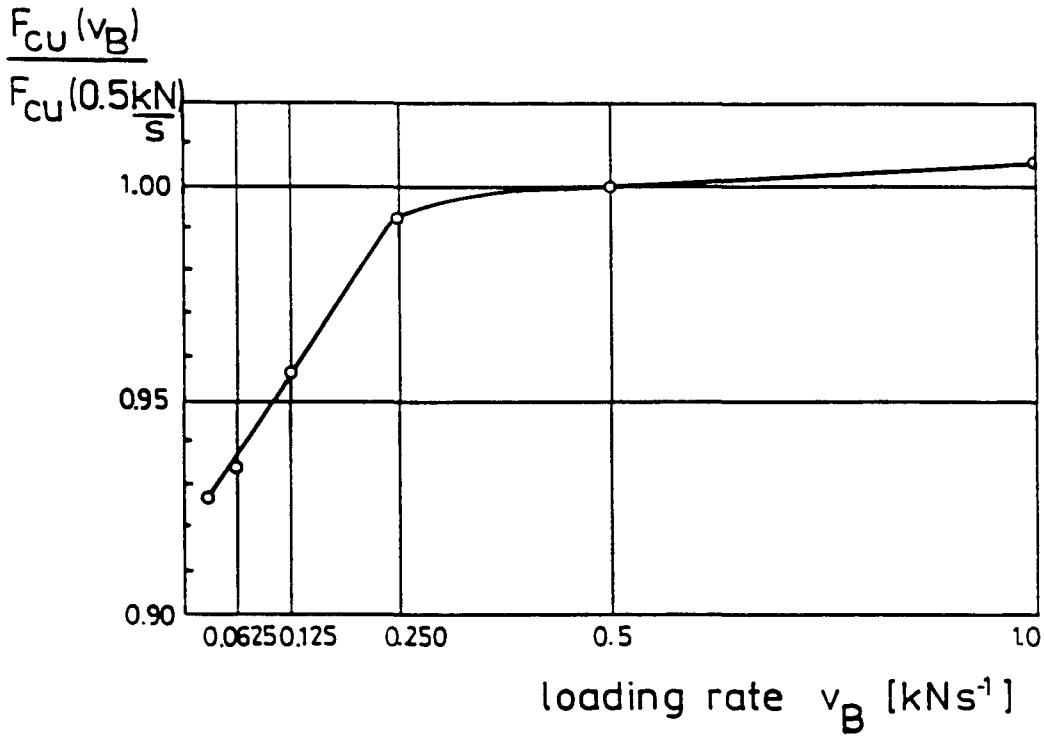

Fig. 2.3: Related Tensile Strength of GFRP dependent on Loading Rate [7]

As can be seen from Fig. 2.3 the influence of the loading rate vanishes for v_B > 0,250 kN/s. For the subsequent tests the value 0,5 kN/s will be chosen. Similar results were obtained for AFRP Arapree strips with a loading rate of 1 kN/s (= 0,42 $^0/_{oo}$/s). In the range of these loading rates no significantly differing results are obtained if the tests were performed with a constant strain rate.

2.1.5 Influence of free length of specimen

Because the strength of the fiber is influenced by the density of flaws along its length, the free length of the test specimen will also play a role for the composite strength. In [8] results for GFRP bars with a variable free length are reported. In Fig. 2.4 the results are depicted. The strength values are normalized to the strength of the length of 300 mm. This value will be chosen for the subsequent tensile tests.

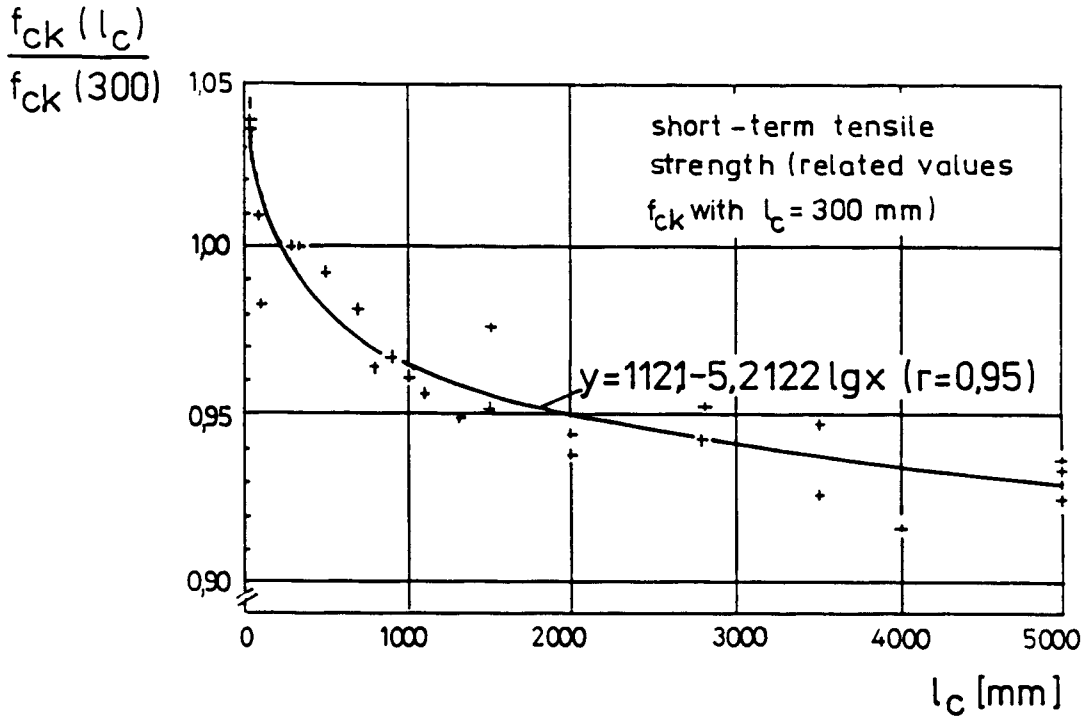

Fig. 2.4: Related Tensile Strength of GFRP Dependent on the Free Length of Specimen [8]

2.1.6 Influence of pre-conditioning

An FRP element is immediately after production completely dry. From then on, it will absorb moisture dependent on the relative humidity of the surrounding air and on the diffusion properties of the matrix resin. Absorption and desorption of moisture are entirely reversible [1]. If the FRP element is - immediately after production - sheathed by a shrunk-on polymeric cover, the up-take of moisture is slowed down.

Tests have shown that due to the storage of as-produced unsheathed GFRP bars at 20 °C/65 % r.h. and the following absorption of moisture a loss of strength of 3,5 % occurs which levels off after a storage time of 8 to 9 weeks [1]. Table 2.1 gives results obtained at different laboratories. For the future test work the FRP material should be preconditioned at the laboratory for a period of about 4 weeks at 20 °C/65 % r.h. prior to testing.

Table 2.1: Influence of the Duration of Preconditioning at 20 °C/ 65 % r.h. on GFRP [9]

laboratory	IWB Stuttgart	Bayer AG	STRABAG
free length (mm)	300	700	910
tensile strength (N/mm^2) at the age of			
0 days	-	1572	-
7 days	1599	1510	1588
4 weeks	1549	1501	1573 (3 weeks)
9 weeks	1543	1485	1572
19 weeks	1548	-	1536
27 weeks	1542	1474	1500

2.1.7 Influence of anchorage

The type of anchorage used for the tensile test is the most important influence for the breaking force of the FRP element. This is due to the pronounced strength anisotropy of ud-FRP elements as schematically shown by Fig. 2.5.

By the anchorage the technical means are understood to introduce the force of the testing machine into the FRP element and vice versa. The current standards do not specify the suitable methods for this task. From Fig. 2.5 is clear that this introduction of force must be realized by compressive stresses acting normal to the element's surface and by shear stresses acting on the element's surface in such a way that the "true" strength is not markedly reduced by the multiaxiality of stresses and the sensitivity of ud-FRP against the latter. The gradual transfer of force is essential.

If the anchorage does not meet the above-mentioned, admittedly only general requirements, the failure of the FRP partly or totally commences at the entry of the specimen's free length into the anchorage. Thereby a part of the element's true strength is lost. An efficient anchorage ensures that the majority of fiber bundles breaks within the free length and not at the entry into anchorage. Fractographic study of the failed specimen becomes an

important tool to judge the efficiency of an anchorage in conjunction with the forecast value of Equ.(2.3).

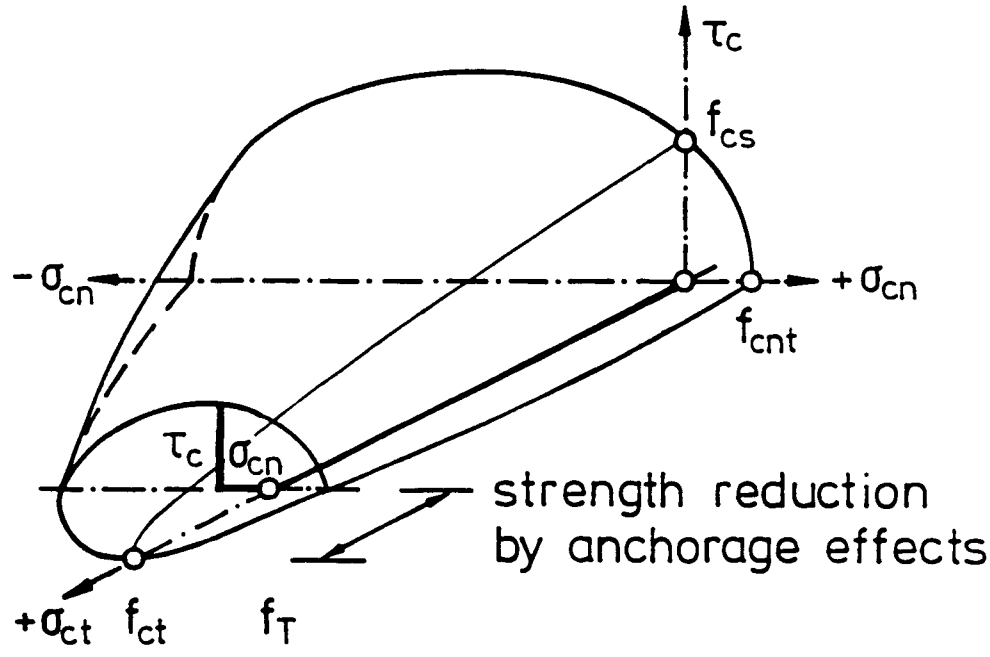

Fig. 2.5: Multiaxial Strength of FRP

The testing of an unprotected FRP element in a tensile testing machine with grooved and teethed steel clamps is completely unsuitable. More suitable are hydraulically or pneumatically adjustable and segmented steel clamps with compressible layers to protect the naked bar from injury. Besides this method it is necessary to have an anchorage of high efficiency not only for the short-term tensile testing but also for the long-term and fatigue testing. This leads to anchorages in which the introduction of force into the bar is reparated from the introduction into the test machine.

The development of laboratory anchorages is today an interactive process of experiments and analytical studies and is strongly based on experience. Three basic types have been developed:

a.) clamp anchorage
b.) wedge-bond anchorage
c.) bond anchorage

The types a.) and b.) will be briefly dealt with. The type c.) is not suitable as laboratory anchorage.

Clamp anchorage

One of the first clamp anchorages using a wedge to clamp the FRP bars was used to test Arapree flat strips. Fig. 2.6 shows this anchorage [10]. The flat strip is anchored within the conical steel housing by two polyamid wedges of great length and with a rectangular groove. The steel housing is then choulder-supported. To enhance friction either the surface of the strip was sanded or intermediary layers were used. Tests [11] showed that it was - especially for elements with a high number of filaments - difficult to impossible to activate the true composite strength. This type of anchorage is well suited for the pretensioning of AFRP elements.

Therefore, as an alternative a clamp anchorage as shown in Fig. 2.7 was developed. Tests with a constant and varying distribution of the clamping forces were performed.

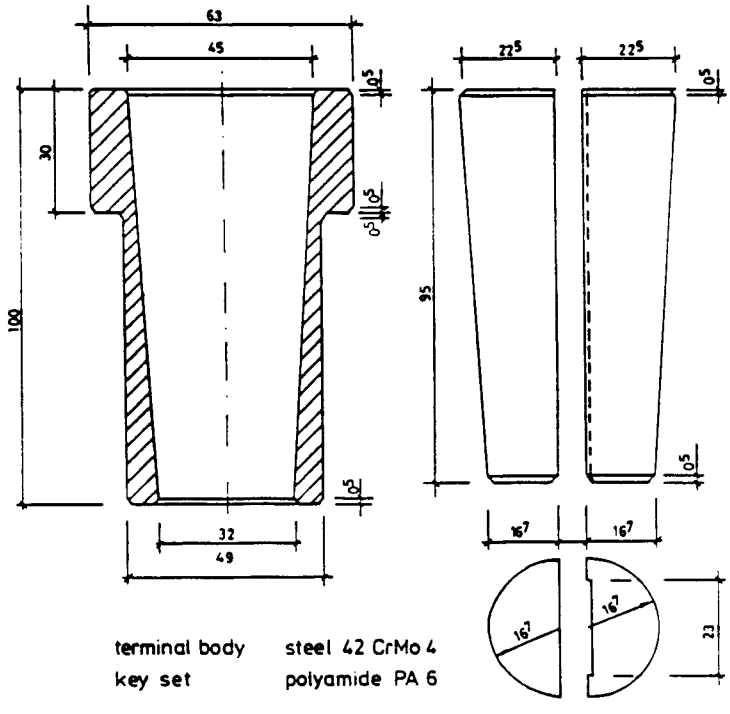

Fig. 2.6: Wedge Anchorage for ARAPREE [10]

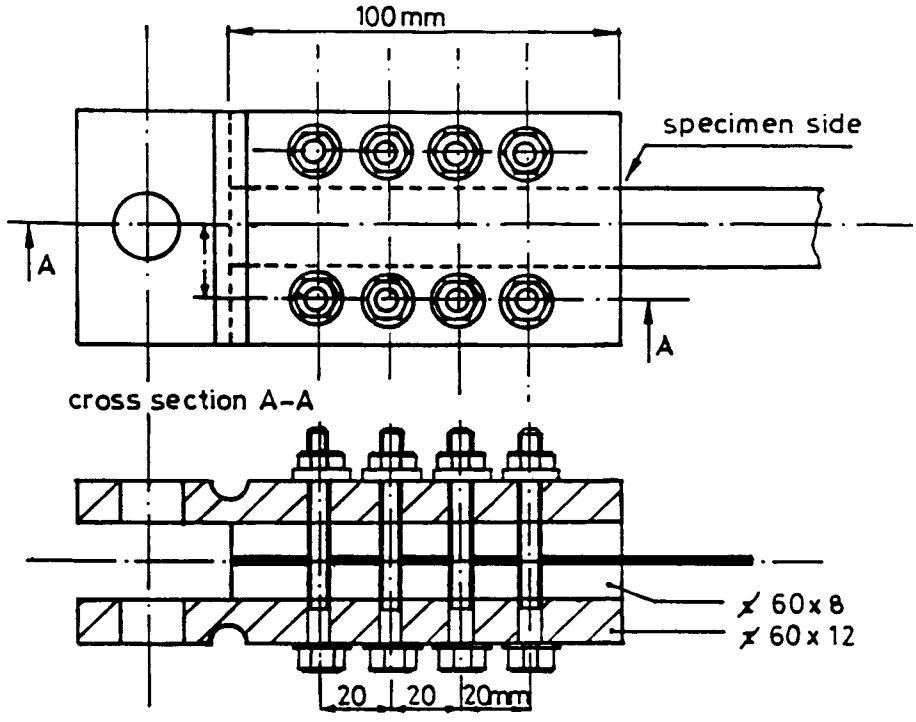

Fig. 2.7: Clamp Anchorage with 8 Bolts for the Testing of ARAPREE Strips [11]

The clamp anchorage was also used by STRABAG and by the IWB, University of Stuttgart to determine the tensile strength of 7,5 mm GFRP Polystal bars [9;12]. Detailed studies were performed to investigate the magnitude and distribution of the clamping forces, the efficiency of intermediary layers and of protective metal sleeves.

Fig. 2.8 shows this anchorage as it is used today. It is described in detail in [12]. The round FRP bar is epoxy-glued in a steel tube of 300 mm length. Transverse pressure is exerted by high-strength bolts which must be precisely tensioned. Steel springs maintain the clamping forces constant. With this anchorage the highest breaking forces with little dispersion could be attained in comparison with other types of anchorage. Handling is difficult and requires high precision.

Wedge-bond anchorage

Although with the clamp anchorage of Fig. 2.8 an anchorage of high efficiency is available it is too cumbersome and not practical for routine tensile testing and long-term testing. This fact lead to the development of the wedge-bond anchorage whose mechanism of force transfer is shown in Fig. 2.9.

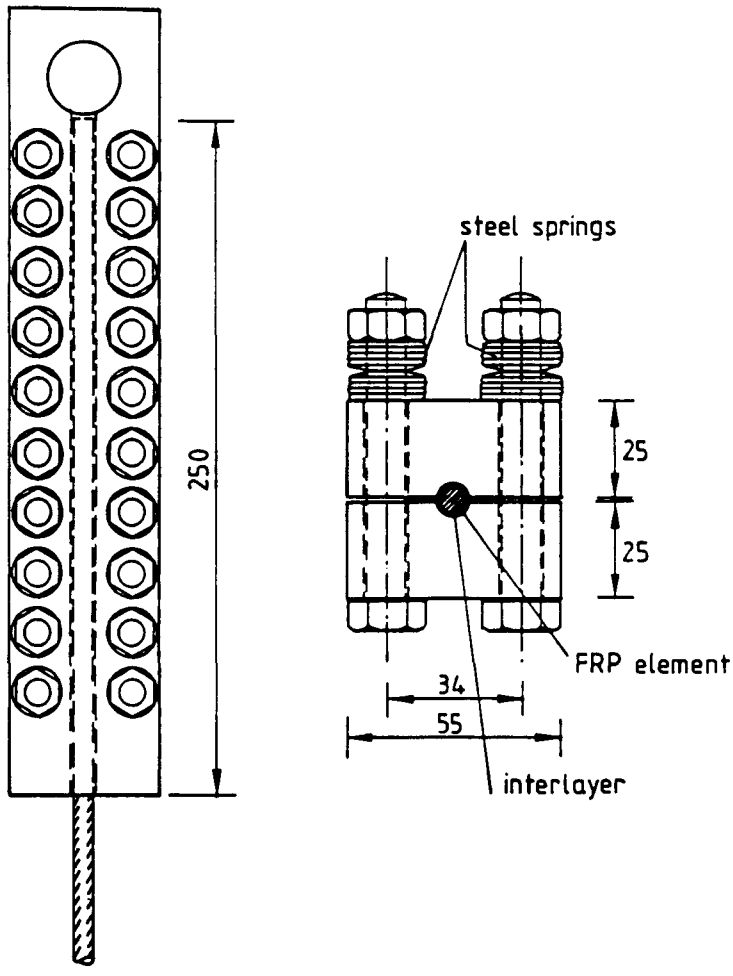

Fig. 2.8: Clamp Anchorage for the Testing of GFRP Bars [12]

As shown in Fig. 2.9, the FRP bar is epoxy-glued on both ends into steel tubes with an inner thread. The steel tubes are then gripped at their rear ends by commercial steel wedges in a conical housing. More details and test results are given in [13]. By this combination of force transfer by bond alone and by bond plus transverse pressure very high breaking forces with a low dispersion of results was attained. This anchorage is equivalent to the clamp anchorage of Fig. 2.8 and by far less cumbersome.

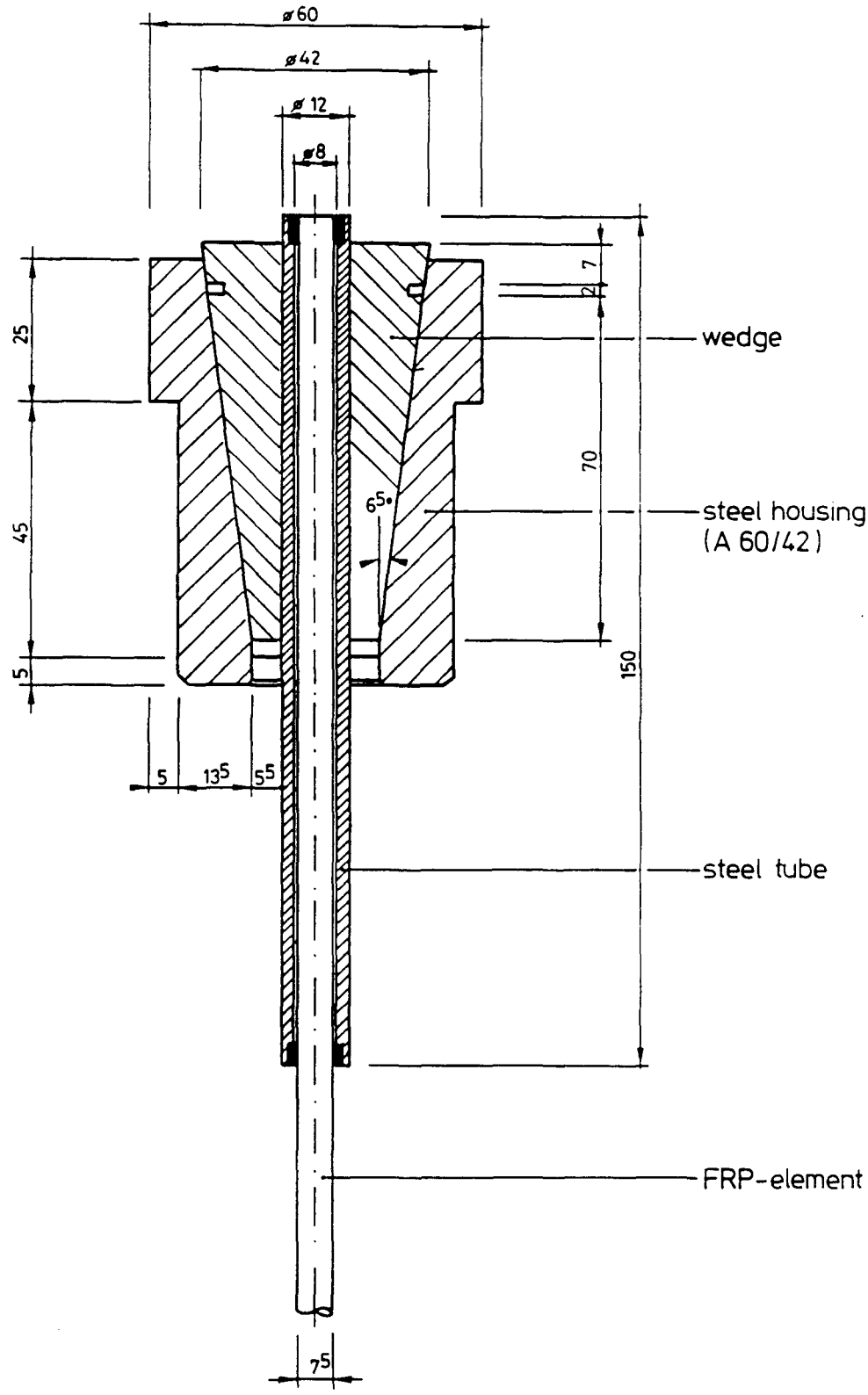

Fig. 2.9: Wedge Bond Anchorage for Testing GFRP

2.2 Short-term Shear Strength

2.2.1 Overview on existing test regulations

Shear tests are used to assess the strength of bond between fiber and resin of an FRP element. In addition to their importance for the generation of design data for structural applications such tests are necessary because they can be employed to assess new sizing systems for the surface treatment. But not only in this respect but also for the characterization of FRP elements these testing methods became important. Ideally the test method should produce only shear. However it is difficult to meet this condition because of coupling effects. Nevertheless several methods for determining the in-plane shear properties of FRP exist in the literature [14;15]. Most of them follow the ASTM - Standard D 2844 [16], which is identical with the European Standard EN 2377 [17] and the DIN 29 971 [18].

2.2.2 Interlaminar shear strength - ILSS

Delamination failures commonly occur in highly loaded composite structures. Several tests have been developed to determine the ILSS, but all have severe limitations. Perhaps the most popular of these tests is the short beam test, which consists of a small unidirectional FRP strip loaded in three point bending. This method based on the elementary beam theory. Experimental work is described in [14;19]. The test set-up is illustrated in Fig. 2.10.

The specimen is supported by two rods; F is the applied load. The compressive roller bearings are exactly defined because the ILSS strongly depends on the ratio l/h (length/height). The stress distribution along the thickness of the FRP element is a parabolic function which reaches a maximum value at the middle of thickness and zero at upper and lower surface. Thus we obtain the ILSS:

$$f_{c\tau i} = \frac{3\ F_{cu}}{4\ A} \qquad (2.4)$$

where F_{cu} is the load at failure, $f_{c\tau i}$ is the ILSS and A is the cross-sectional area.

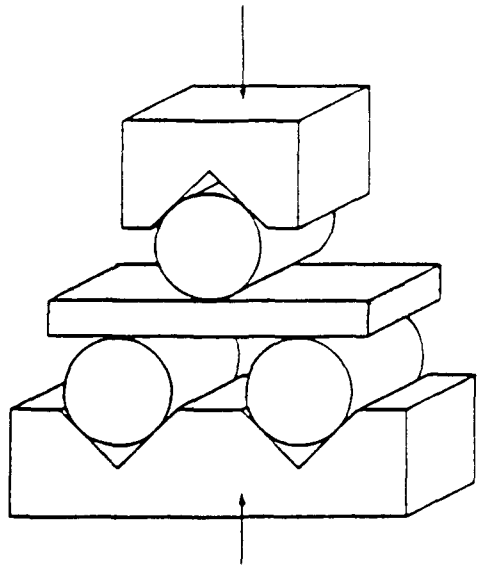

Fig. 2.10: Schematic Test Set-Up for Short-Beam ILSS [19]

A comparison with results of other kinds of shear stress tests [15] shows that the values reached by the short beam test are approximately 20 % higher than those measured by the torsion shear test or other tests. The latter are not regarded in this report.

In [19] ARAPREE elements with a fiber volume of 40 % and a filament number of 100.000 were subjected to a short beam test.

In [19] also results of ILSS tests were compared for composites with glass-, aramid- and carbonfibers. The values are described as a function of the ratio l/h for unidirectional composites of 60 % fiber volume. It is recognizable that the AFRP shows the lowest value in comparison to the others. Altogether the ILSS values appear much higher as in other publications [14]. Usual the ILSS range between 35 MPa and 45 MPa. Generally, it is to remark that this kind of test is not recommendable because coupling effects influence the test results.

With the investigations of shear strength as routine check for GFRP it was necessary to find a simple testing method. So in connection with [20] a new method was described which was used firstly for the determination of the ILSS of glassfiber composites with a round cross section. It was called "punching test". This kind of test is not mentioned in standards. In this test, from a 10 mm rod section a punch-out is performed with the help of a

topping slab. The applied failure force-divided by the surface of the punched-out cone-corresponds to the ILSS. The test set-up which was used is shown in Fig. 2.11.

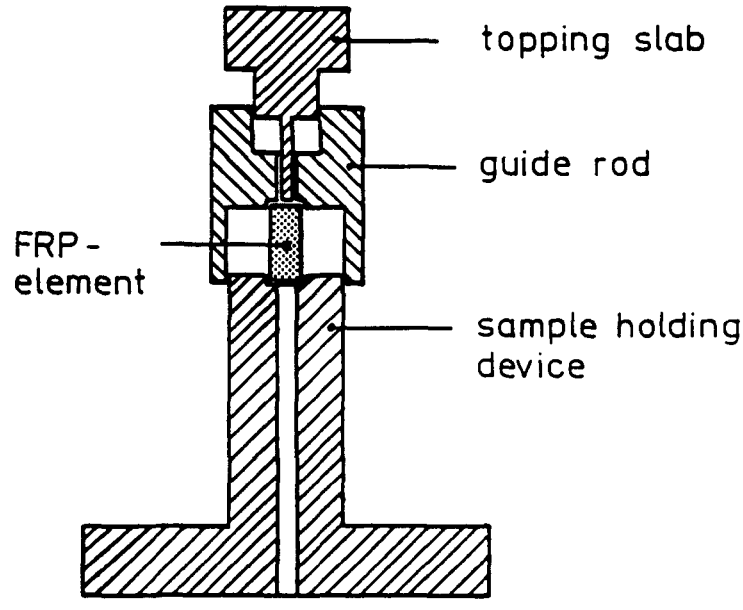

Fig. 2.11: Punching Test Set-up for Determining ILSS of GFRP

In Fig. 2.12 the relation between the shear strength along the cone and the displacement is depicted. Up to the ILSS there is a linear relation between the ILSS and the displacement. Failure occurs by an in comparison lower displacement.

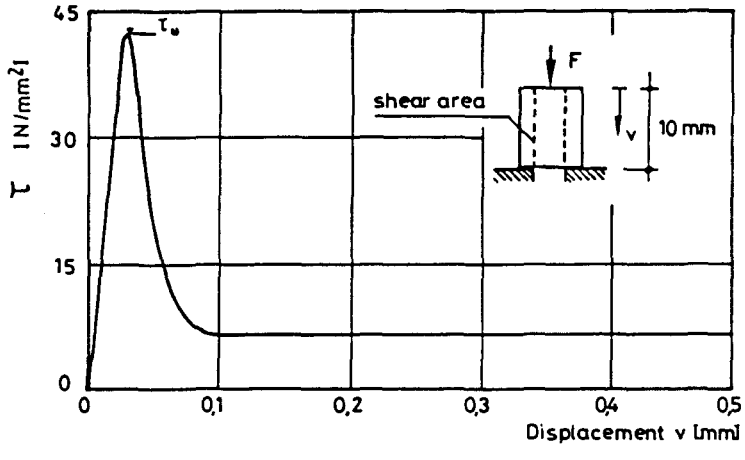

Fig. 2.12: Relation Between ILSS and Displacement of GFRP [21]

More details of this test (loading rate, specimen length) are given in [21]. It is important, that the tests are performed carefully because of the sensitive test set-up.

2.2.3 Surface shear strength

The quantification of the force transfer between the fiber containing core and its outer coating which may consists of either the same of a different resin is reffered to as surface shear strength. This property of FRP will also influence the transfer length.

The bond strength is very important for the force transfer between the FRP element and the steel tube or housing of a post-tensioning anchorage. The definitions of the various types of bond strength are illustrated as follows:

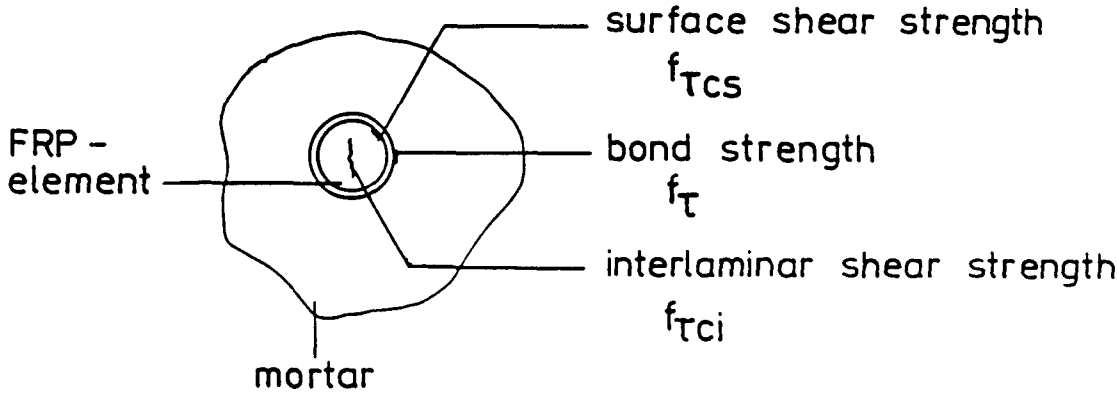

Mostly the surface shear strength is determined by "pull-out" tests (Fig. 2.13). Thereby the FRP element is loaded by a tensile force and similar to the ILSS the pertinent displacement will be recorded. The results are presented as shear stress-displacement diagrams.

Within the scope of tests with GFRP [22;23;24] a mean surface shear strength $f_{\tau cs}$ of 30 MPa was measured for bars embedded in a sand-resin mortar. As the bond failure occurred at the contact surface of the bar with the mortar all other strength values were in excess of $f_{\tau cs}$.

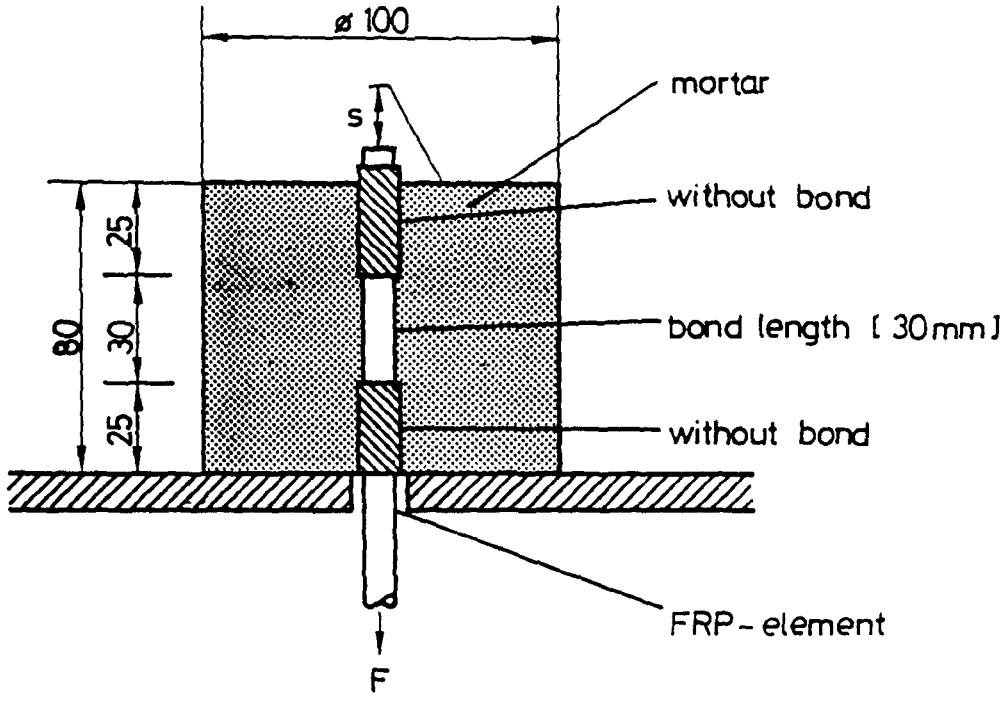

Fig. 2.13: Pull-Out Test Set-up for Determining Surface Shear Strength [22]

The surface shear strength and the chosen test method are not the object of any standard. Also in the literature only a small number of publications exist. Further research is necessary.

3. EXPERIMENTAL DETERMINATION OF MECHANICAL LONG-TERM PROPERTIES

3.1 Introductory Remarks

Besides the static short-term strength of FRP under axial tension, several long-term properties are of vital importance if FRP are to be used for r/c- and p/c-structures. These mechanical long-term properties comprise:

- creep and relaxation under stresses and strains on the service load level;
- creep rupture strength;
- fatigue strength;
- strength retention.

In this report creep and relaxation of FRP are not dealt with. Emphasis is put upon the creep rupture (often also called stress rupture) and the fatigue behaviour. Strength retention is the residual static tensile strength of an FRP element which was subjected to a precedent long-term static or dynamic tensile test.

3.2 Creep Rupture Strength

In view of the fact that the creep rupture behaviour of FRP tensile elements and the present state of the art have already been dealt with in the Brite-Euram Technical Report 1-1992 [1], only a condensed overview is justified.

If an FRP tensile element is stressed with a certain fraction $0 \leq \alpha \leq 1$ of its static tensile breaking force F_{cu} which is kept constant it will eventually fail. High forces $\alpha \cdot F_{cu} = F_{cl} = \text{const.}$ will be carried for short periods t_u of time, low forces are combined with greater values of the endurance time t_u. This phenomen is called creep rupture, as creep strain is built-up in course of time and due to the constant force. The micromechanics of the creep rupture has been dealt with in several papers [25-34]. In Fig. 3.1 the plot of the long-term forces F_{cl} versus the failure times t_u for a certain force level $\alpha_{im} = F_{cli}/F_{cm}$ or $\alpha_{ik} = F_{cli}/F_{ck}$ for several types of FRP and for various environments is depicted. It is the aim of these tests to determine the endurance lines $F_{clm}(t_{um})$ and of $F_{clk}(t_{uk})$ for

long periods of time. Fig. 3.1 shows that the scatter of endurance times t_u is significant. Consequently, an adequate number of tests on the specific force level α_i becomes necessary to establish the above-mentioned endurance lines with a required confidence level.

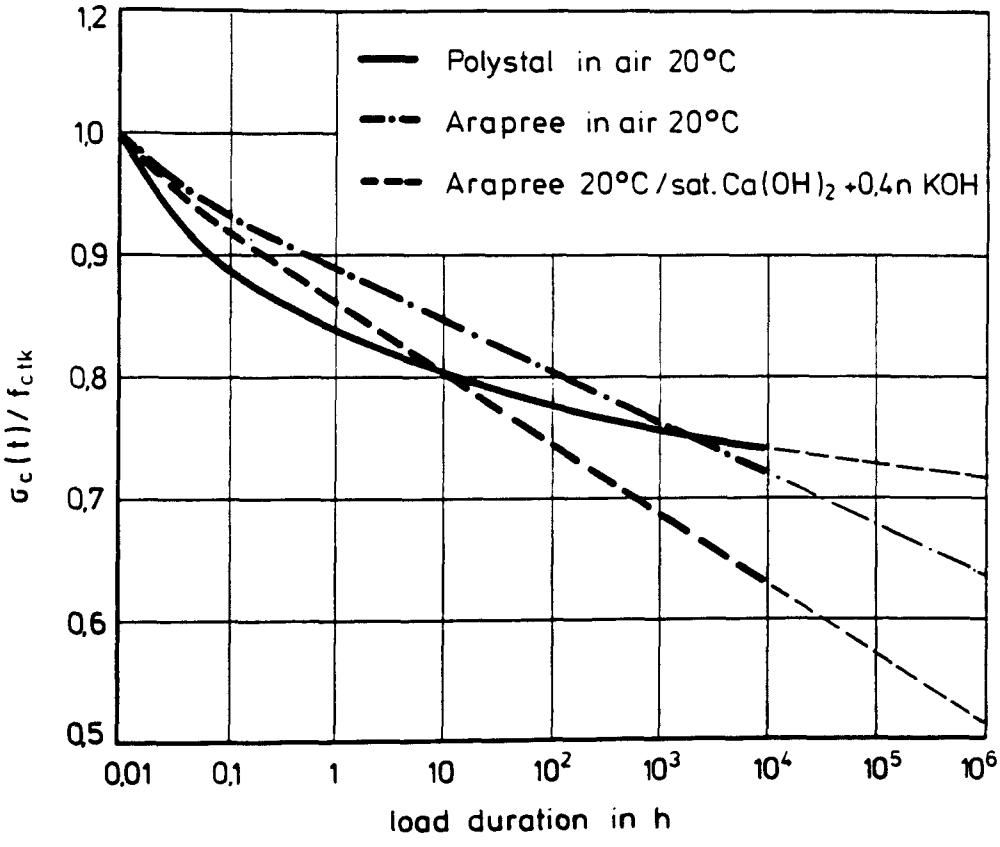

Fig. 3.1: Creep Rupture Lines of FRP Elements

There is only little experimental evidence available with respect to the creep rupture behaviour of commercial FRP tensile elements. Fig. 3.2 shows the mean creep rupture lines for GFRP bars of different cross-section at an environment of 20 °C/65 % r.h..

For 10^6 hours (≈ 114 years) the mean creep rupture strength F_{clm} (10^6 h) ≈ 0,70 F_{cm} can be estimated.

For GFRP and AFRP the environment is of great influence on the creep rupture strength. Especially the alkaline environment of fresh concrete and of the pore solution of hardened concrete has to be studied for GFRP and AFRP bars if these are to be used for pretensioned or for cement-grouted ducts

of post-tensioned concrete members. Only for AFRP bars of the ARAPREE type extensive experiments have been performed. Nothing is known for CFRP, although a high resistance can be expected.

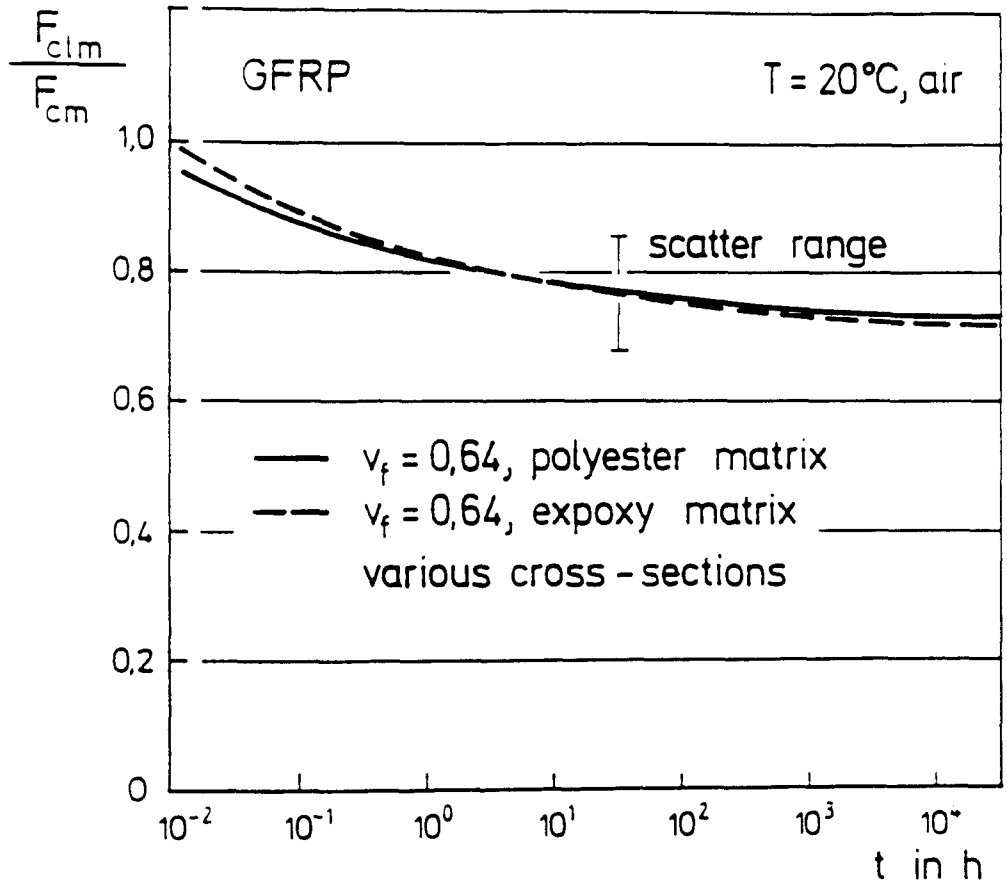

Fig. 3.2: Creep Rupture Lines of GFRP Bars [32]

In Fig. 3.3 the results of tests performed at Delft [49] with ARAPREE flat strips with 100.000 TWARON filaments subjected to an alkaline solution of sat. $Ca(OH)_2$ + 0.4 n KOH, pH 13 and the statistical survival lines acc. to [1] are shown.

The hollow circles mark tests which were terminated before the creep rupture of the specimens in order to test the strength retention of the latter. The results are shown in Fig. 3.4. One may observe that the residual axial tensile strength of these specimens whose creep rupture failure was obviously imminent scatters significantly.

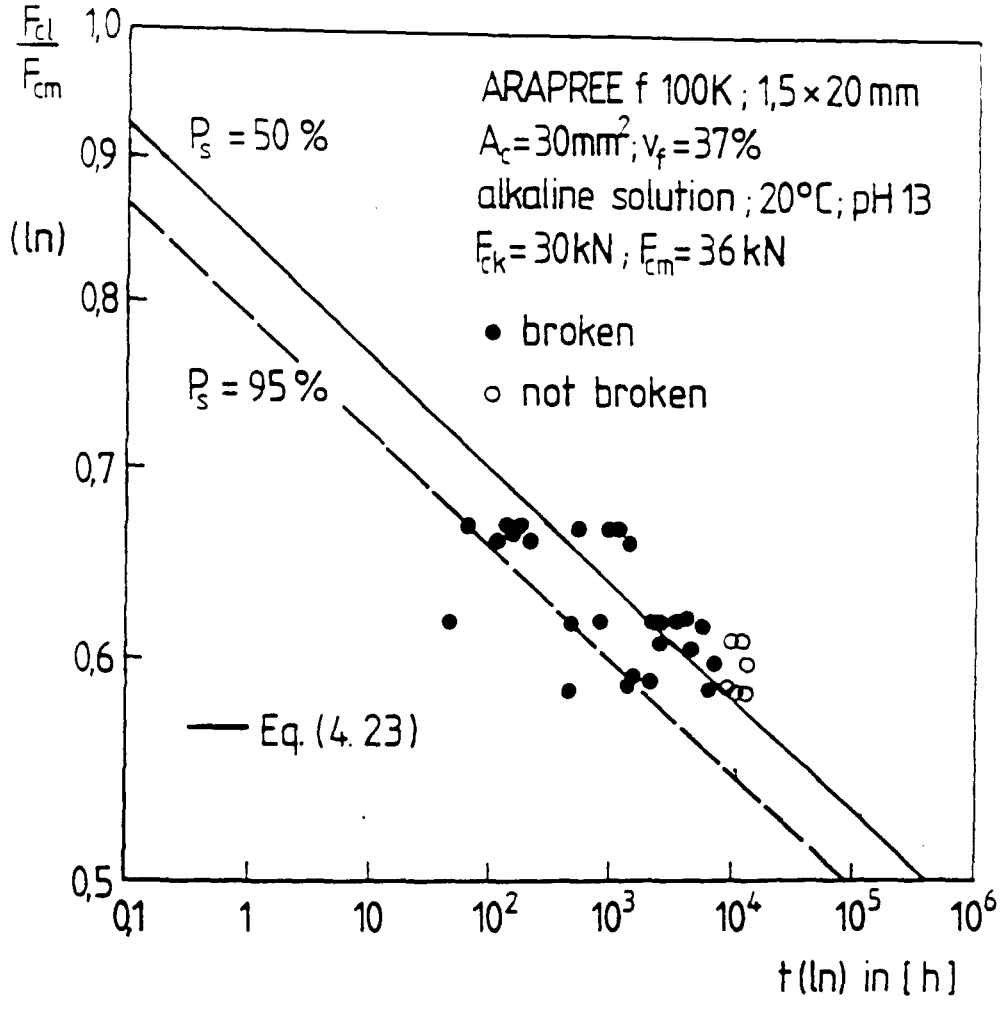

Fig. 3.3: Creep Rupture Tests of ARAPREE Flat Strips in Alkaline Solution [35]

The most extensive tests were carried out by [35-37]. Resin-impregnated S-glass and aramid fiber bundles were used. Test times were up to 10^4 hours. Especially the methodology of test evaluation will serve here as guideline in connection with the theoretical forecast models of the sources [38-42].

The evaluation of the scarce experimental data necessitate extensive testing of the creep rupture behaviour.

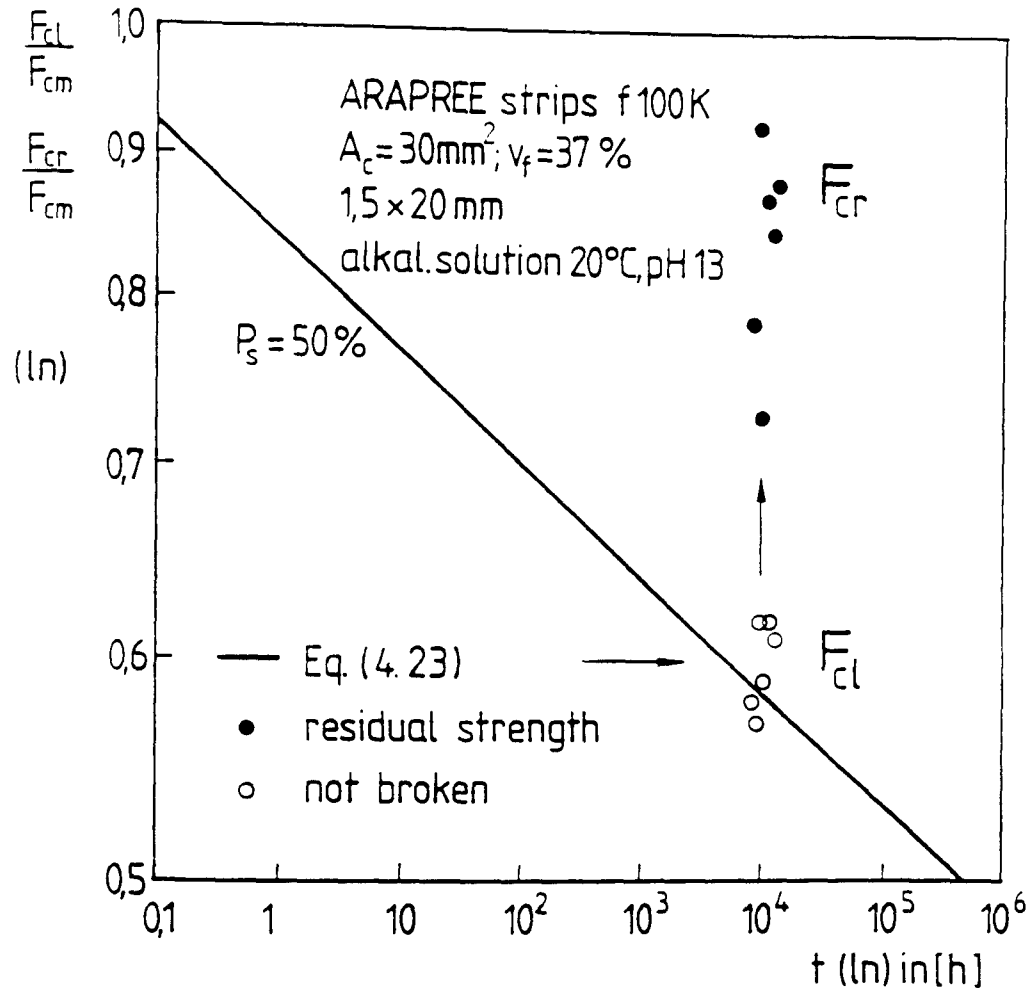

Fig. 3.4: Strength Retention of ARAPREE Flat Strips After Long-term Loading in Alkaline Solution

3.3 Fatigue Strength

For the application of FRP for r/c- and p/c-structures especially the fatigue behaviour in axial tension is of relevance. In contrast to reinforcing or prestressing steel the stress range $\Delta\sigma_c = \sigma_{co} - \sigma_{cl} > 0$ decreases steadily with increasing number of load cycles. Hence, no limiting value $\lim \Delta\sigma_{cu}$ exists.

The micromechanics of fatigue failure has been studied by several authors [43-49]. It is similar to that of creep rupture failure. The fatigue strength of an FRP tensile element is suitably determined for a constant upper stress σ_{co} corresponding to the admissible axial prestress adm σ_c which has to be determined on basis of the characteristic creep rupture

line $F_{clk}(t)$ for the time range of the service life. Hence with the constant force

$$F_{co} = \sigma_{co} \cdot A_c = \text{adm } \sigma_c \, A_c \tag{3.1}$$

and the variable lower force

$$F_{cl} = \sigma_{cl} \cdot A_c < F_{co} \tag{3.2}$$

the S-N-lines with an adequate number of identical tests for the specific force range $\Delta F_c = F_{co} - F_{cl}$ can be experimentally determined.

The fatigue strength of FRP elements depends on a series of parameters. First of all the type of fiber is of great influence. CFRP have the highest fatigue strength, with that of AFRP being only slightly less. The fatigue strength of GFRP is significantly lower. Fig. 3.5 shows fatigue test lines (mean values) from [50]. The type of matrix resin is of influence. Progressive matrix cracking seems to be detrimental.

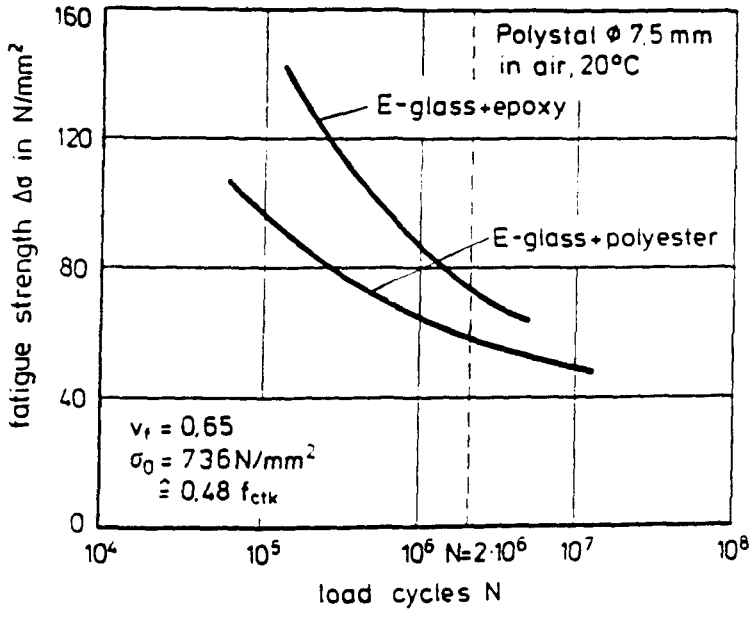

Fig. 3.5: Fatigue Behaviour of GFRP Polystal Bars Dependent on Matrix Resin [50]

Fig. 3.6 shows the results of fatigue tests performed with CFRP rods (Leadline, Japan) with a constant stress ratio $R = \sigma_{cl}/\sigma_{co} = 0{,}1$

(20 °C/65 % r.h.). The fatigue strength, expressed as stress range at $N = 10^7$ of $\Delta\sigma_c \approx 1.1$ GPa = 0.60 f_{ck}, is extraordinarily high.

Nothing is known about the fatigue strength of FRP when exposed to an alkaline environment.

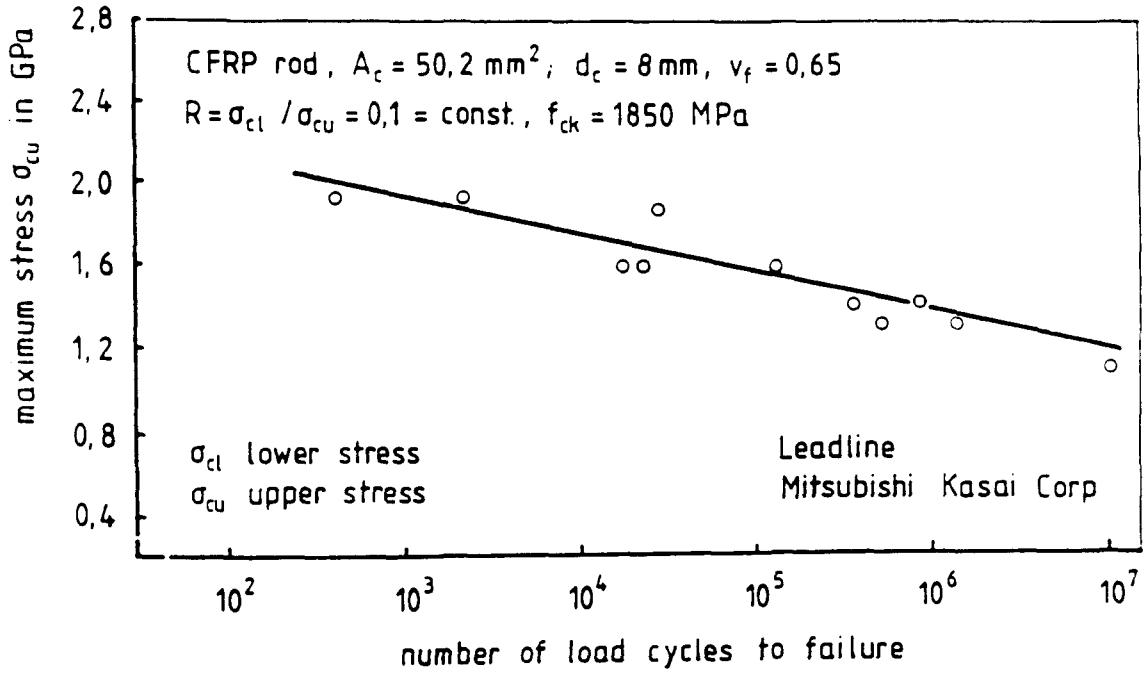

Fig. 3.6: S-N-Line of CFRP Rods (Leadline)

Again the evaluation of the existing experimental data proves that extensive fatigue testing of FRP is essential.

4. TEST METHODS OF IBMB FOR THE DETERMINATION OF MECHANICAL PROPERTIES OF UNIDIRECTIONAL-FRP-ELEMENTS

4.1 Short-term Tensile Testing

4.1.1 Main requirements for the test set-up and testing procedures

Because of the great significance of the short term tensile strength for the quality control and for the classification of the FRP-material the test set-up have to meet several requirements:

- a suitable anchorage must be available, s. 2.1.7
- pre-conditioning of the FRP-bars prior to testing is necessary, e.g. four weeks at 20 °C and 65 % r.h.
- an approved tensile testing machine according to DIN 51 300 and ISO 5893 must be available.

4.1.2 Testing machine

All tests were performed in a conventional tensile testing machine "Zwick 1498" with a maximal tensile force of 100 kN. Various grips allow the testing of several kinds of anchorages. Fig. 4.1 and 4.2 show the testing machine with measuring devices.

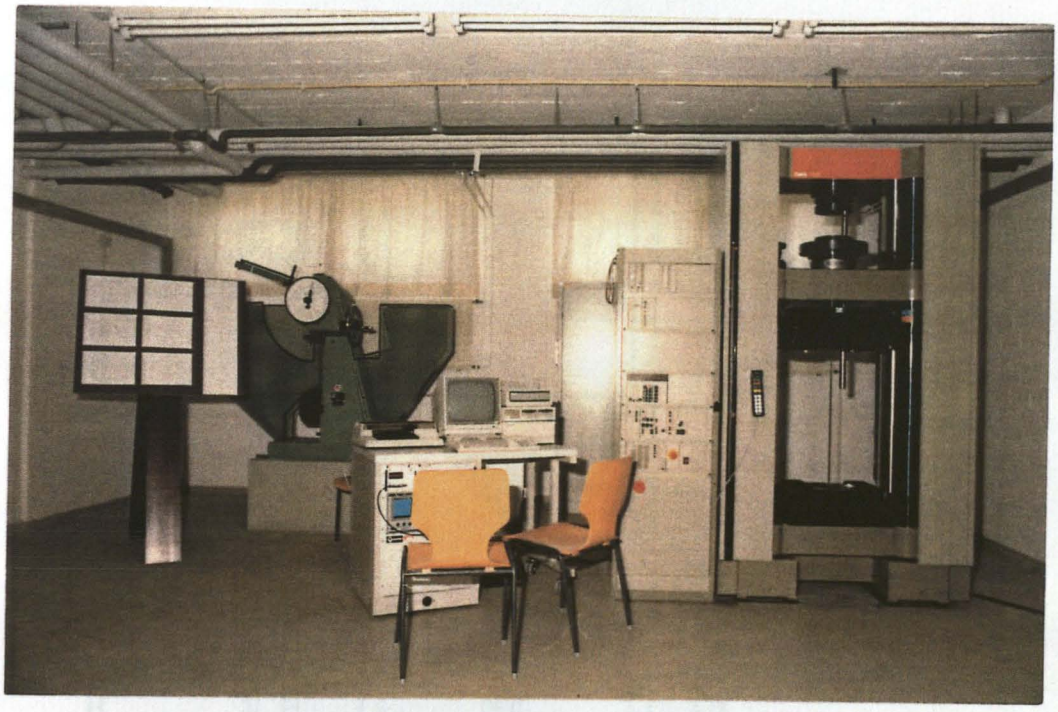

Fig. 4.1: Tensile Testing Machine "Zwick 1498"

4.1.3 Anchorage assembly

For the short-term tensile testing two kinds of anchorage systems are used at the iBMB: the clamp anchorage and the wedge-bond anchorage, both are described in chapt. 2.1.7. Extensive research has been performed to optimize the dimensions of the components and the structure of the anchorages.

4.1.4 Loading device

The specimens are subjected to a tensile force with a constant loading rate, i.e. 0.5 kN/s, alternatively 5 mm/min.

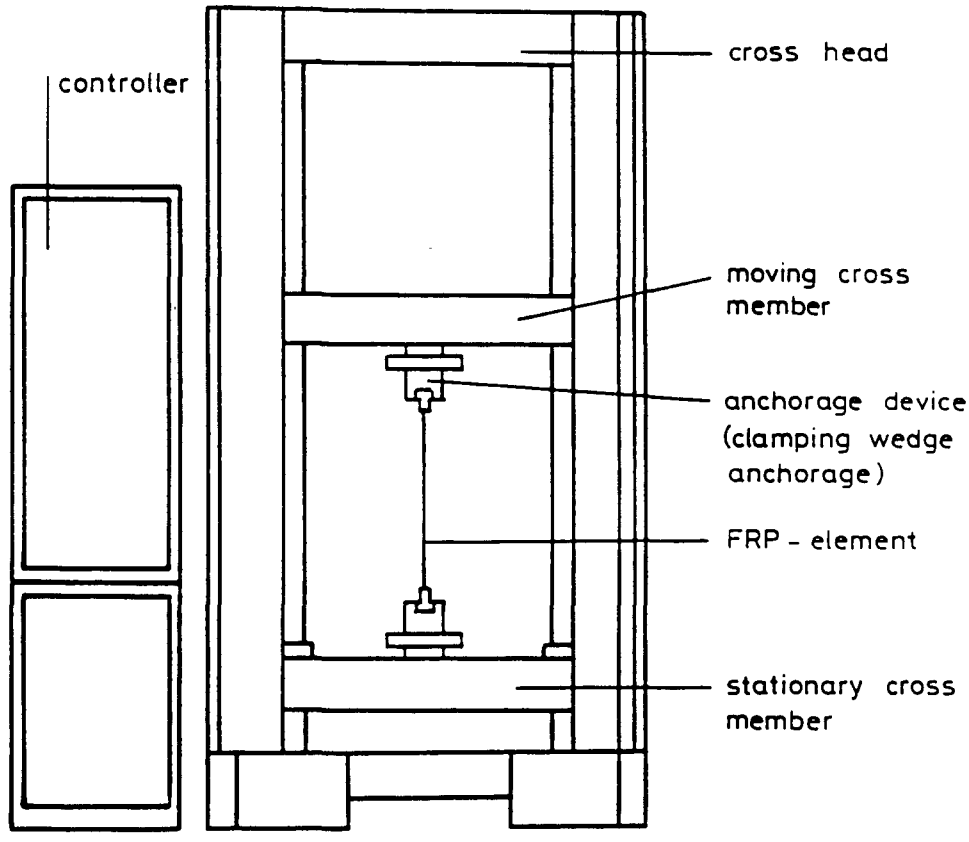

Fig. 4.2: Testing Device

4.1.5 Measuring devices

The measurement of the axial tensile force and the corresponding deformation of the specimen are performed continuously until failure occurs. The test data are recorded on a personal computer. Some specimens are fitted with strain gauges (5 mm) on their free length and on the steel housing of the wedge-bond anchorage to record deformations.

For the determination of the modulus of elasticity the axial deformation is measured with two LVDT W5E.

4.2 Creep Rupture Testing

4.2.1 Main requirements for the test set-up and testing procedures

The test set-up and the measuring devices for the determination of the creep rupture strength of an FRP tensile element have to meet several requirements:

- static long-term forces - in the same magnitude as the static short-term tensile breaking force - must be generated and maintained constant over a long period of time. Control and adjustment of force must be possible,
- the initial axial strain and the time-dependent creep strain must be recorded reliably and accurately during long-term testing,
- a single bar anchorage with a high static efficiency factor must be available so that the creep rupture strength of the FRP element is not influenced by anchorage effects,
- the FRP element shall be subjected on a certain part of its free length to an environment similar to the future conditions in practice.

4.2.2 Test frame

The test frame is a closed frame made of structural steel profiles Fe 360, s. Fig. 4.3 and 4.4. The frame consists of two vertical columns and two cross-heads, which are inserted between the columns and fastened by high-strength prestressed bolts. The testing of specimens with a variable length is possible. In all ten frames were built and positioned in a laboratory with 20 °C/65 % r.h. at the iBMB, TU Braunschweig. The frame is designed for a permanent force up to 100 kN.

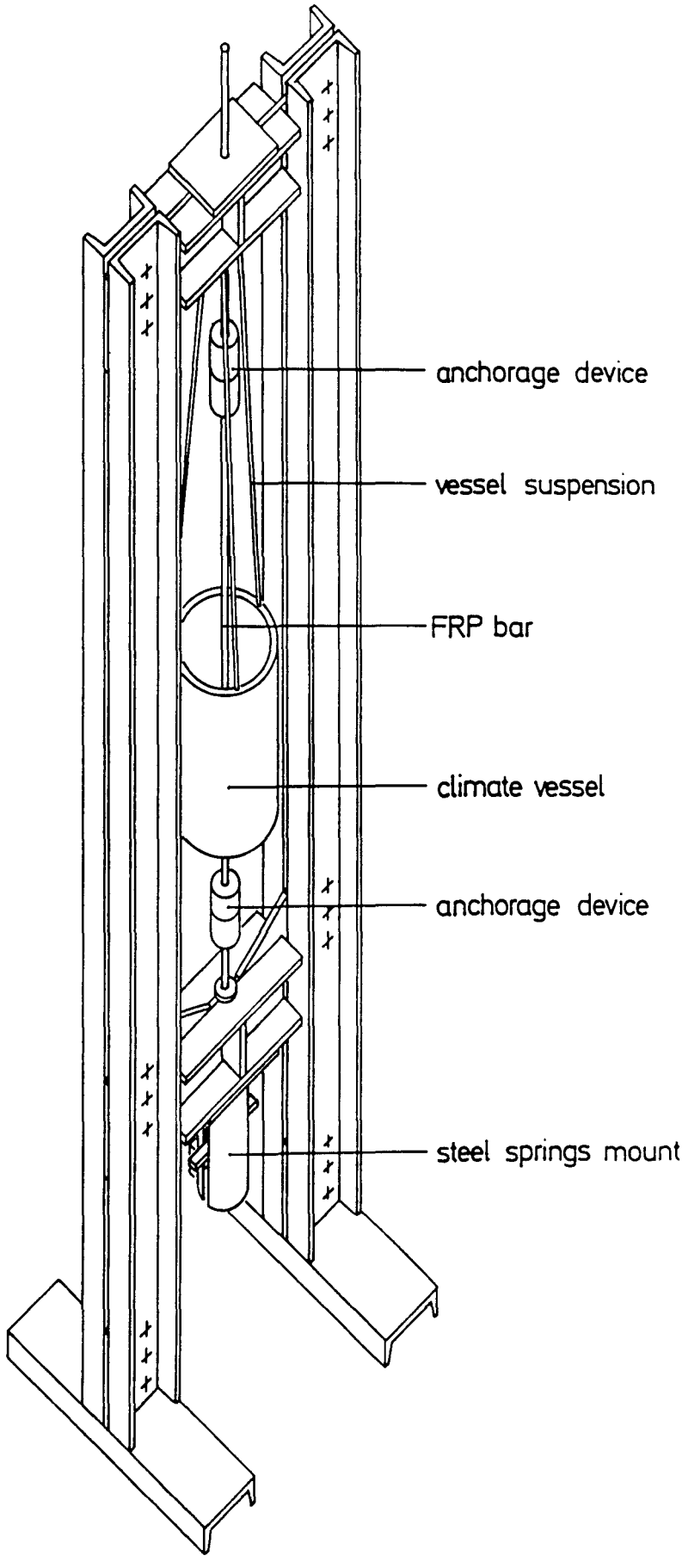

Fig. 4.3: Test Set-Up for Testing FRP Elements

Fig. 4.4: Photograph of Test Set-up

4.2.3 Anchorage assembly

The selected FRP test specimen has a circular cross-section. It is fitted on both ends with suitable anchorages. The anchorage consists of several components. The bar is glued on both ends into steel tubes with an inner thread to improve the resin-bond action. Fig. 4.5 shows the steel tube for a circular FRP bar with a diameter of 7.0 to 7.5 mm. With the FRP bar being now protected against direct transverse pressure and injury, tubes are gripped by conventional wedges which are placed in the steel housing with an inner cone. The steel housing rests - via circular brackets - on another steel cylinder which is closed by a circular steel plate by six screws. The load is introduced into the steel plate by a tension rod which is screwed into the boring. Fig. 4.6 shows the drawing and Fig. 4.7 the photograph of

the anchorage. The steel rod is the force-transmitting element which passes through a hole in the cross-head on both ends.

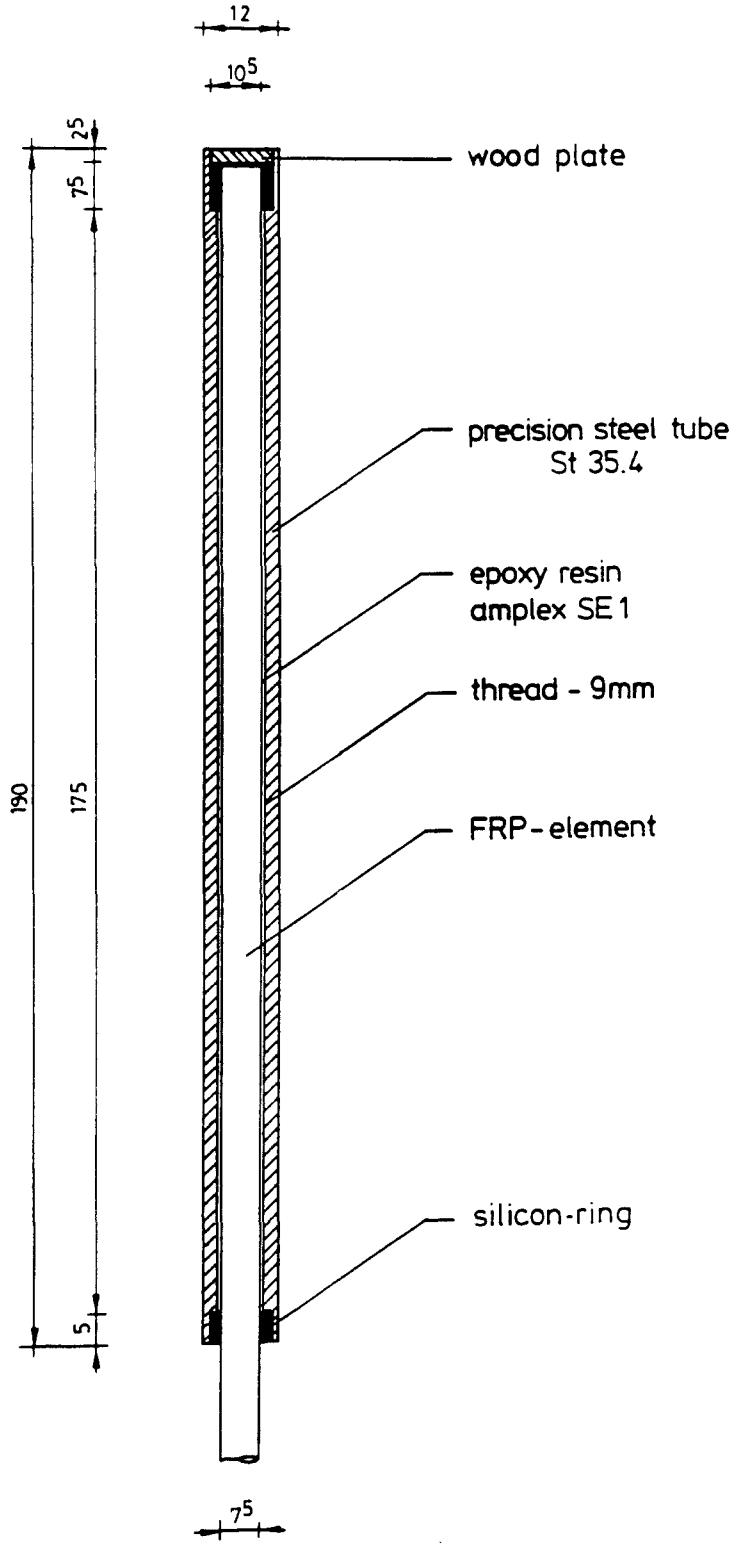

Fig. 4.5: Steel Tube for Protection and Gripping of Specimen

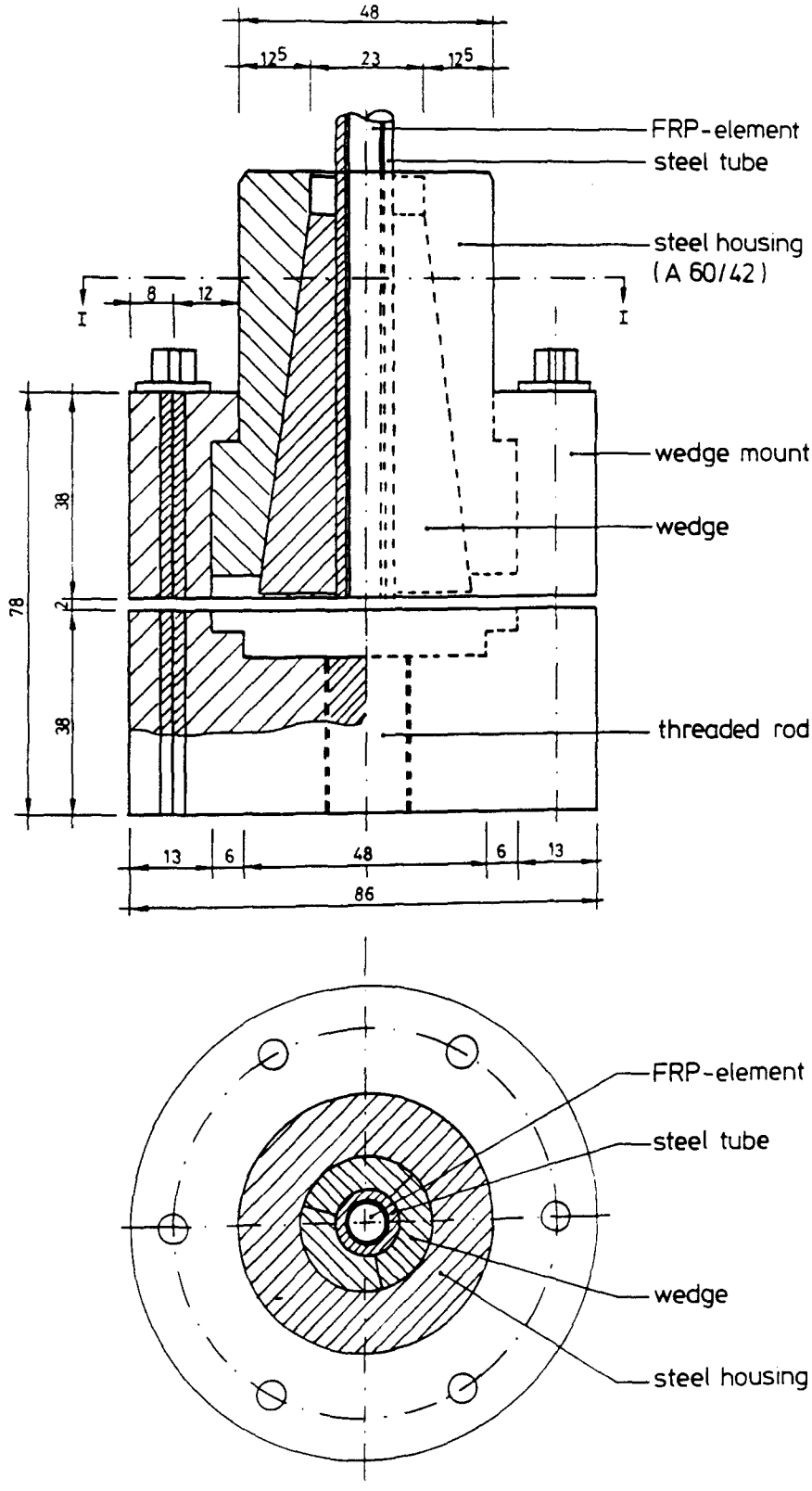

Fig. 4.6: Anchorage Device

Fig. 4.7: Photograph of Anchorage Element

4.2.4 Loading device

The specimen is stressed at the upper cross-head by a hydraulic jack with a center hole. The jack is seated on a jack chair to permit the tightening of the nut on the bar, until the desired force is attained. The force - during initial loading and at each readjustment of force - is measured with a load cell. The loading rate is 0.5 kN/s. Fig. 4.8 and 4.9 show the loading device. Once, the force is attained the jack and the load cell will be removed after an initial observation period of 24 hours.

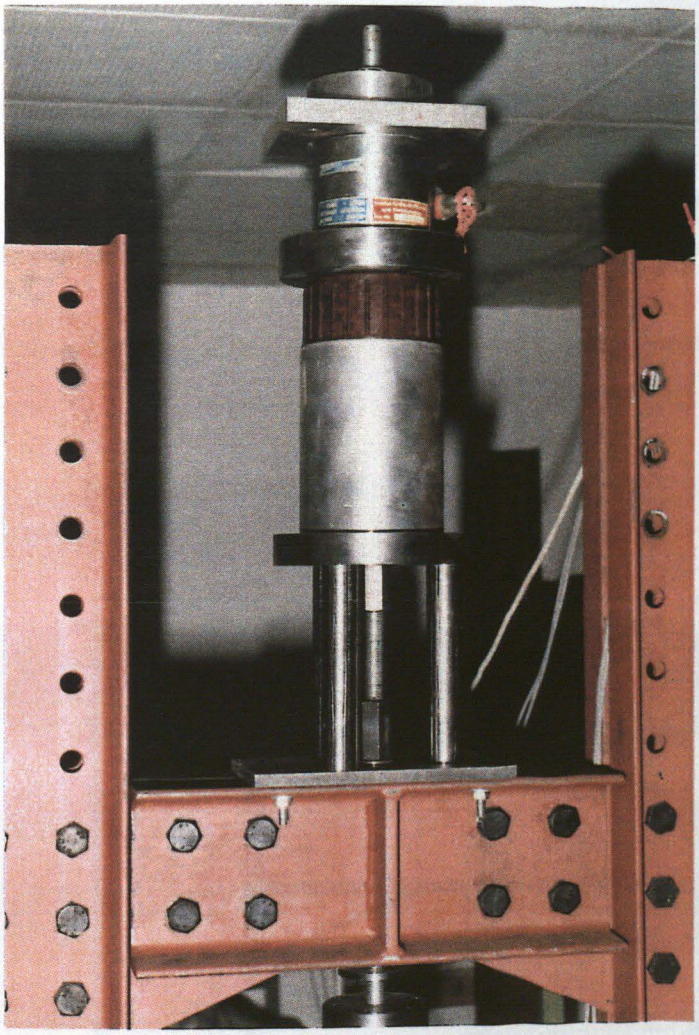

Fig. 4.8: Photograph of Loading System

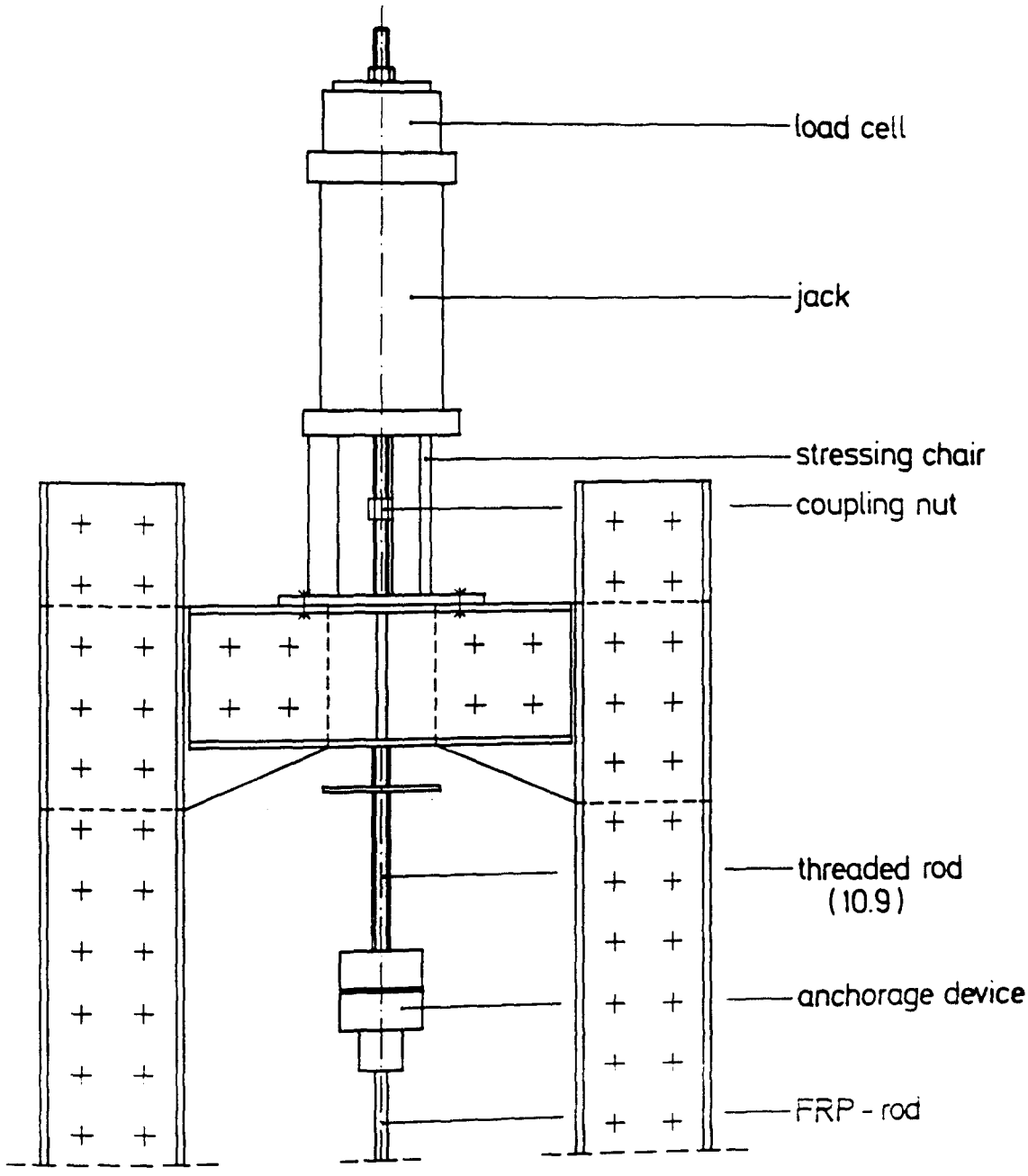

Fig. 4.9: Loading System

4.2.5 Springs

Load constancy during the testing time is attained by a package of plate springs, s. Fig. 4.10. The actual spring package is enclosed by a steel cylinder tube. Fig. 4.11 shows the calibration line of the chosen spring package.

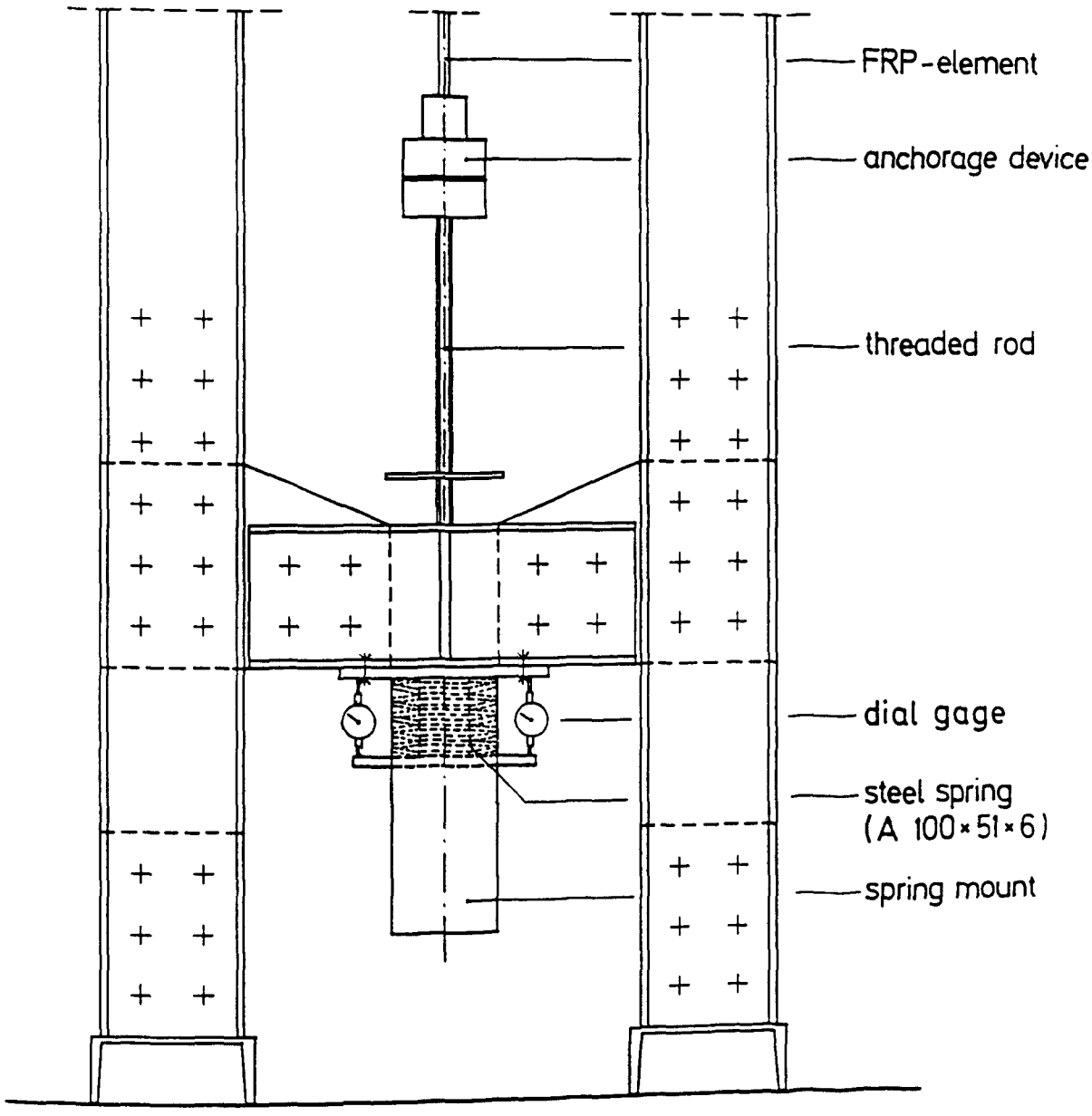

Fig. 4.10: Load Constancy by Steel Plate Springs

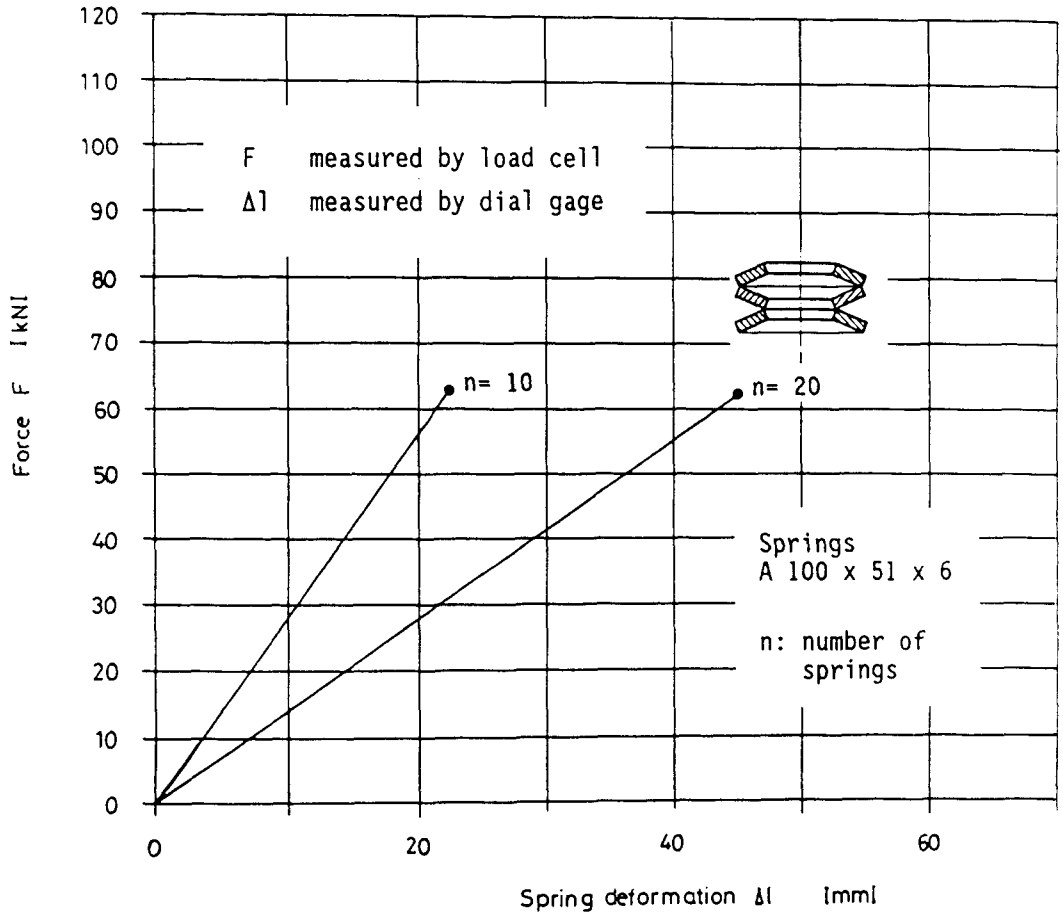

Fig. 4.11: Calibration Lines of Springs (A 100 x 51 x 6)

In course of time the spring package will extend due to the specimen's creep. The magnitude of extension serves for the control of load constancy. Consequently, the extension is measured on two sides with 1/100 mm dial gages. It is planned to complete this measuring system with an LVDT. If the force falls still to a specified lower boundary value readjustment is necessary and possible.

Pilot tests have proved the suitability of this equipment. Testing according to the test program has commenced.

4.2.6 Measuring devices

The measuring devices for the force and the spring deformation have already been described. The measurement of the axial tensile strain of the specimen is performed by two LVDT W5E (total displacement 5 mm) of H&B Meßtechnik

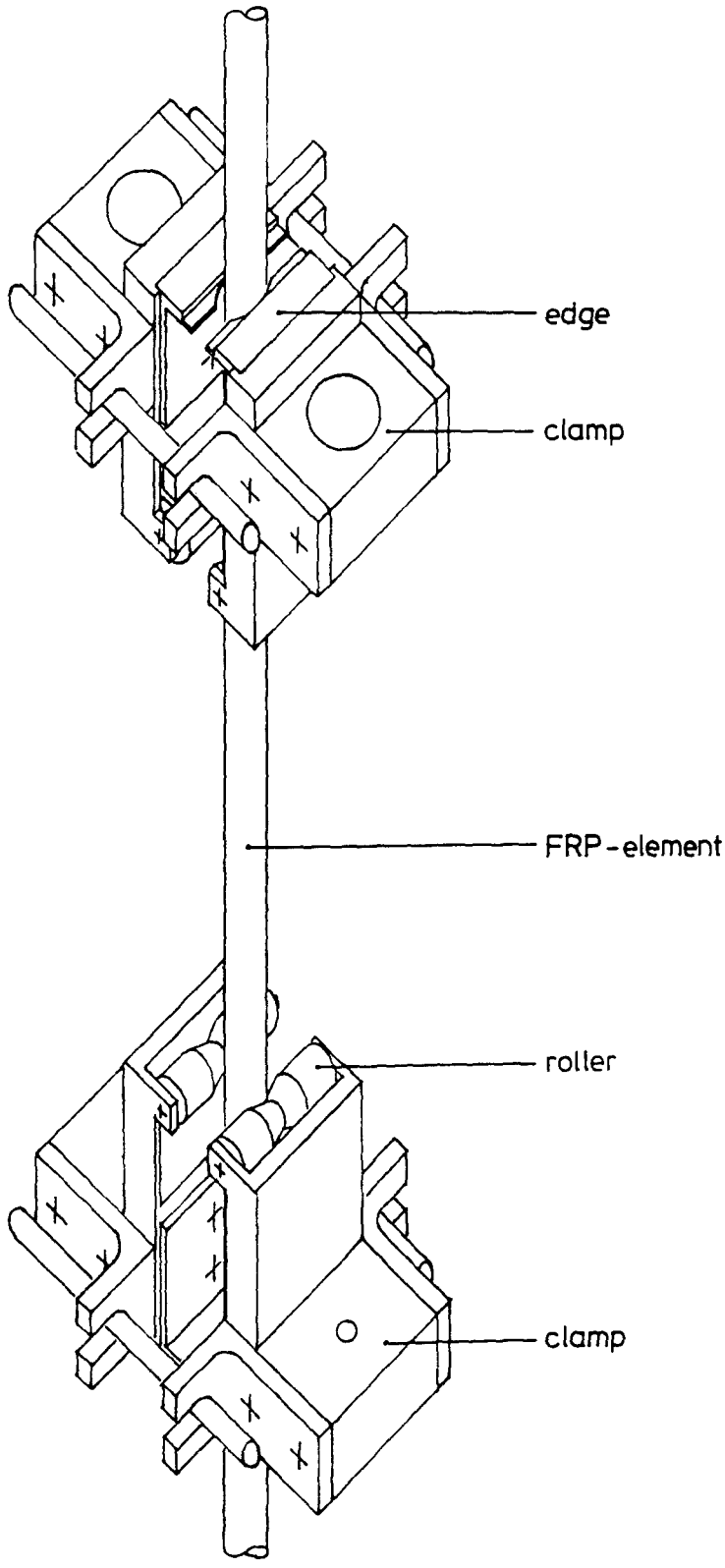

Fig. 4.12: Set-up of Deformation Measurement in the Free Length of the Specimen

over a gage length of 200 mm. The gage length is situated within the environment vessel. The bridging of the gage length is performed with bars made from invar steel whose thermal dilatancy is negligible. The upper ends of the invar bars are coupled with the plungers of the LVDT.

Fig. 4.12 shows a principal drawing of the measurement set-up. The device consists of two clamps with rollers and edges, made from Cr-Ni-steel. The clamping force and the edges were chosen in such a way that the bar is not adversely injured (control by SEM investigation was performed).

The electric signals of the LVDT are recorded with a data measurement and aquisition system (H&B), and then evaluated and stored on floppy disc. Each test can be controlled independently and automatically. Break-down of one measuring device or of the electric current does not influence the acquired data. Fig. 4.13 shows the set-up for data recording.

Fig. 4.13: Data Recording and Acquisition Set-up

4.2.7 Test Environment

Several types of environmental conditions will be investigated. The influence of normal dry condition of 65 % r.h. and 20 °C can be studied easily.

For the investigation of the influence of the concrete pore solution on the creep rupture behaviour a special environment was choosen.

The pore solution of concrete contains several ions: Na^+, K^+, Ca^{2+}, OH^-, SO_4^{2-} and others. At the age of 28 days the concentration of ions has nearly stabilized [51;52]. In order to simulate the high aggressivity of the natural pore solution, an aqueous saturated solution of $Ca(OH)_2$ + 0.4 n KOH was choosen [26]. This solution exhibits a pH value of about 12 at 20 °C.

The solution is stored in a cylindrical vessel made from HDPE, s. Fig. 4.14. It consists of the container and the lid, both having a central boring for the FRP specimen. The specimen is positioned axially in the vessel. It is on a length of L_t = 250 mm in direct contact with the solution. Within L_t the gage length L_e is situated.

The vessel is suspended from the upper cross-head. Both holes (bottom and lid of vessel) are sealed in such a way that neither a leakage of the solution nor an ingress of air (carbon dioxide) can occur. At certain time intervals the pH value will be controlled and the solution will be stirred.

4.3 Fatigue Testing

4.3.1 Main requirements for the test set-up and testing procedures

The test set-up and the measuring devices must meet the following requirements:

- the upper force F_u and the lower force F_l must be maintained constant until failure of the FRP bar occurs,
- the axial strain must be recorded continuously or automatically at the upper and lower force at defined load cycles,
- the single bar anchorage must be designed in such a way that fatigue failure does not propagate from the anchorage,
- the FRP test specimen shall be subjected on a certain length to the specified environment.

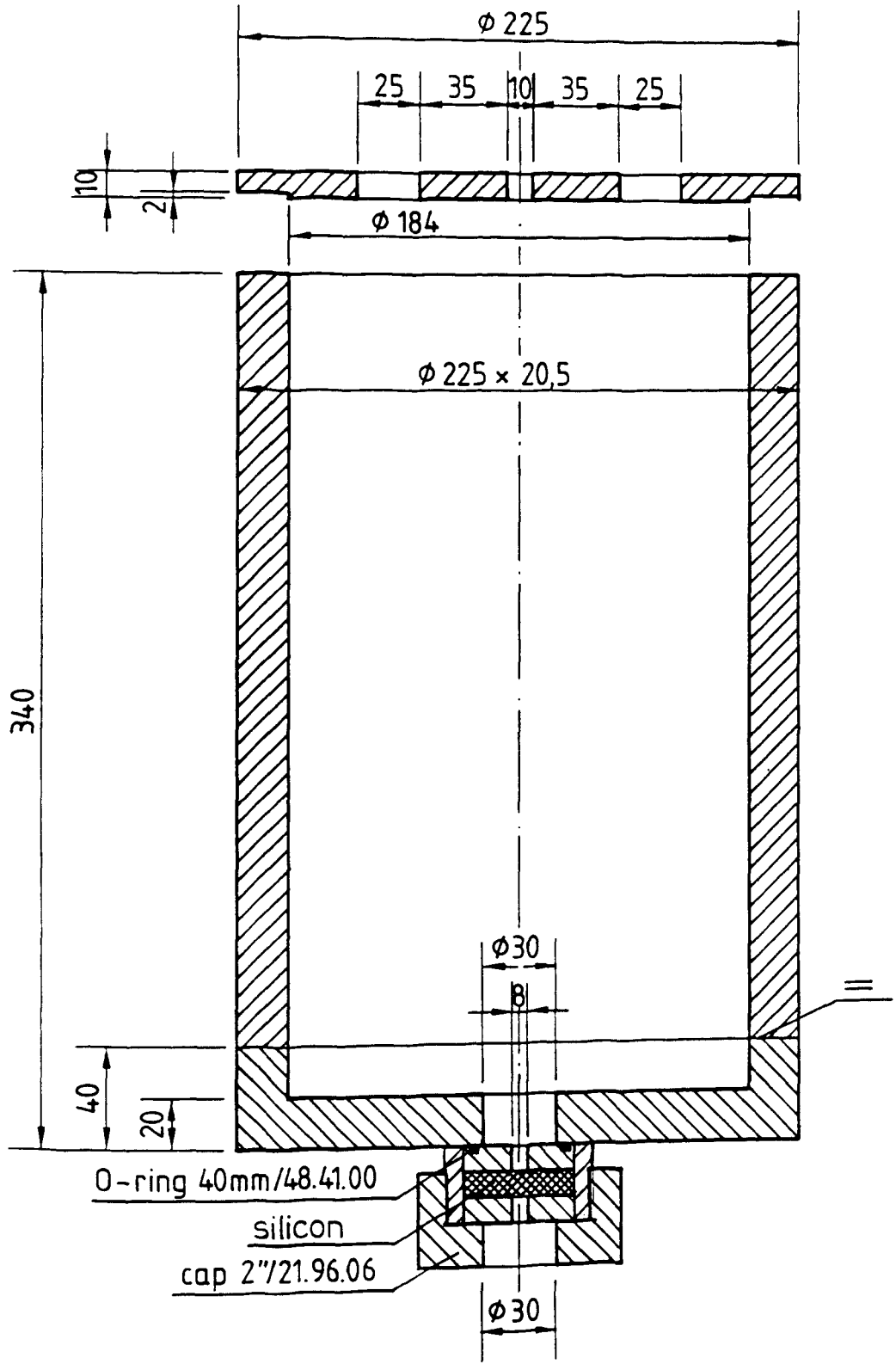

Fig. 4.14: Environment Vessel

4.3.2 Test frame and anchorage

In all three test frames were built. They are designed as shown in Fig. 4.15. The same anchorage elements as for the creep rupture testing were chosen.

4.3.3 Loading device

The loading is performed hydraulically with a jack of 100 kN force-controlled at the lower cross-head. The jack has a central hole to accommodate the threaded steel tension bar which is connected with the lower anchorage of the specimen.

Fatigue loading is performed with a frequency of about 5 Hz. The loading is controlled and measured by a 100 kN load cell (± 0.5 kN).

4.3.4 Measuring devices

Because of the vibrations during fatigue testing a measuring system with LVDT used for creep rupture testing is not suitable. It is planned to use electric strain gages, situated on the free length, which have to be sealed from contact with the solution. In addition slip of the bar at its entry into the anchorage and deformations of the steel housing will be measured.

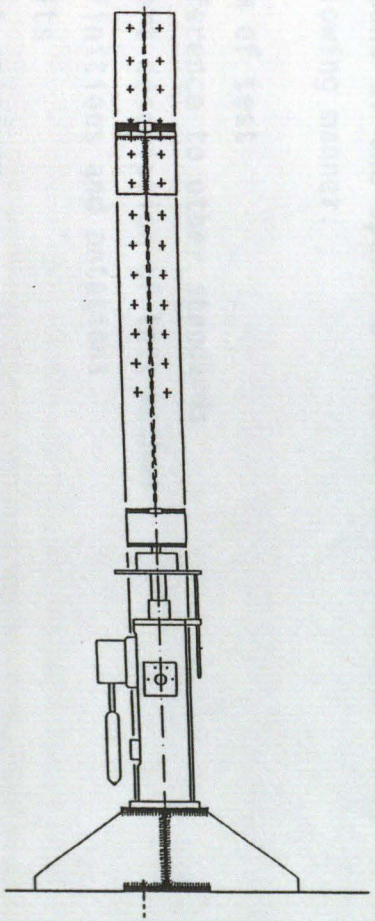

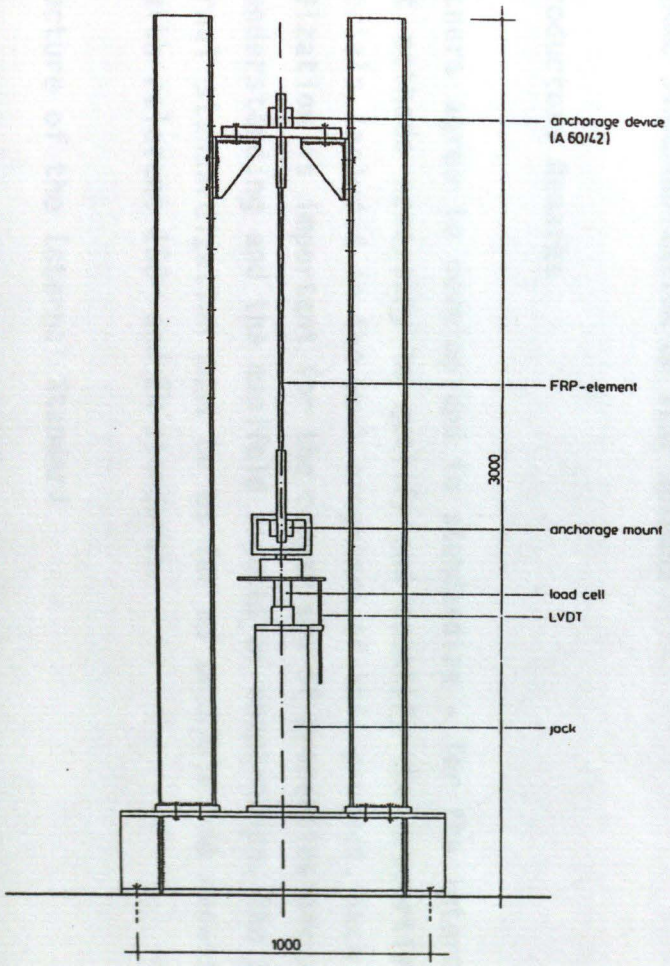

Fig. 4.15: Test Frame for Fatigue Testing (Photograph - Side and Front View)

5. INTERNAL STANDARDIZATION OF TEST METHODS

5.1 Introductory Remarks

The partners agree to develop and to standardize - for the internal use - the test methods necessary to qualify and quantify the properties of the FRP materials included in the work programme of this project. Such internal standardization is important for the comparison of properties etc., for the mutual understanding and the manifold aspects of cooperation. The structure of internal standardization must be as far as possible and necessary congruent with relevant ISO- and EN-standards.

5.2 Structure of the Internal Standard

The content of the specific internal test standard should be structured in the following manner:

1. Aim of test
2. Reference to other standards
3. Short description of test method
4. Definitions and notations
5. Units
6. Test specimen
7. Cross section of the composite
8. Accuracy of testing an measuring devices
9. Miscellaneous information
10. Test performance
11. Evaluation of test results
12. Test report

5.3 Internal Standard for Short-term Tensile Testing

1. Aim of test

It is the aim of the test to assess the short-term static tensile strength of FRP-elements.

2. Reference to other standards

ASTM D 3039; ISO/DIS 527; DIN 53 455; EN 61; Product-specific test regulations of the FRP producers.

3. Short description of test method

The specimen is subjected to a tensile force. The force until fracture and affiliated deformations of the specimen are recorded.

4. Definitions and notations

L	total length of specimen
L_c	free length between anchorages
L_e	gage length for measurement of axial strain
F	force (in general)
F_c	short-term tensile breaking force
F_{cm}	mean short-term tensile breaking force of the investigated lot of FRP-elements
ε	strain (in general)
ε_c	strain of composite
ε_m	ultimate strain
σ	stress (in general)
$\sigma_c(t)$	stress at time t

5. Units

Force	N, kN
Stress	MPa, N/mm^2
Strain	$^0/_{oo}$, %
Displacement	mm

6. Test specimen

Shape and dimension

Shape and dimension of the test specimen correspond to the produced state of the FRP-elements.

Total length, test length and gage length

The test specimen has a total length L adequate for the gripping by sleeves in the testing machine of 900 mm and by wedges of 600 mm. The free length is 300 mm.

Initial material data

The specimens have to be from the same production lot. The fiber volume v_f and the density of the fibers ρ_f must be announced by the producer.

Sampling and pre-conditioning of specimen

Samples are cut from coils or rods of the same production lot and are then stored for at least 14 day prior to testing at 20 °C/65 % r.h.

7. Cross-section of the composite

The circular cross-section of the FRP-element is determined by its diameter. If it is necessary the load-carrying cross-section of the FRP-element is determined by weighing the specimen with the length L_t and then calculated with the fiber volume v_f and the density of the fiber ρ_f. Also other shapes of cross-section can be tested.

8. Accuracy of testing and measuring devices

The testing machine must satisfy the conditions given in ISO 5893 [53]. The testing machine shall incorporate a suitable load cell to measure the total tensile force. The used load cell shall indicate the load with an accuracy of at least 1 % of the actual value.

9. Miscellaneous information

If needed other data or information must be gathered.

10. Test performance

Testing machine

The test will be performed in a convential tensile testing machine. The testing machine must satisfy the conditions given in ISO 5893. The specimen is axially loaded with the tensile force F_c.

Anchorage

The specimen shall be gripped on both ends in such a way that the original tensile breaking force of the FRP-element is not markedly reduced. The clamping system shall not cause premature failure at the grips.

Clamp anchorage (Fig. 2.8)

The anchorage consists of two clamping steel plates, which incorporate a steel tube. Transverse pressure is created by prestressed bolts. Load constancy is reached by steel springs (A 20 x 10.2 x 1.1). The material of the steel tube (300 mm) is a special steel (St 35.4) with an inner thread of 9 mm in which the FRP is glued into by an unfilled, two componentical resin (Amplex SE 1).

Wedge-bond anchorage (Fig. 2.9)

The anchorage consists of two parts; a conventional clamping wedge anchorage in combination with a steel tube of 190 mm. The FRP-element is encased in a tighty fitting, resin filled steel tube which is gripped by steel wedges. The basis of the used anchorage is a sleeve, a standard product of the German company PAUL.

Loading

The specimen has been pre-conditioned prior to testing at 20 °C/65 % r.h. The specimen is subjected to a tensile force until failure occurs.

Force and strain measurement

Force is measured with a load cell during the test. The corresponding axial strain is measured with LVDT or with strain gauges glued to the specimens surface. The measurements will be performed continuously until failure.

Number of specimen and evaluation of test results

A minimum of 10 test specimen will be tested for each material to determine characteristic values for the short-term tensile strength. For the evaluation of test results only specimens will be used which are obviously broken on the specimen free length, i.e. between the anchorages.

11. Evaluation of test results

The stress values are calculated on the basis of the initial cross sectional area of the test specimen.

A statistical evaluation of the test results, e.g. mean values, standard deviations and 95 % confidence intervalls shall be calculated.

12. Test report

The test report must contain the following informations:

- complete identification of the material (type, manufacturer, method and date of manufacturing, production lot, shape, dimension, method of preparing etc.)
- complete description acc. to 5.3.1 - 5.3.11)

5.4 Internal Standard for Interlaminar Shear Strength Testing

1. Aim of the test

It is the aim of the test to assess the interlaminar shear strength of the FRP-specimens.

2. Reference to other standards

ASTM D 2344; EN 2377

3. Short description of the test method

The determination of the interlaminar shear strength bases of a so called "punching test". In this test from a 10 mm rod section a punch-out is performed with the help of a topping slab. The applied failure force correspond to the interlaminar shear strength between fibers and matrix of the specimen.

4. Definition and notations

F	force (in general)
F_u	ultimate force
d	effective diameter of the topping slab
L	total length of specimen
$f_{\tau ci}$	interlaminar shear strength

5. Units

Force	N, kN
Stress	MPa, N/mm^2
Displacement	mm

6. Test specimen

Shape and dimension

Shape and dimension of the test specimen correspond to the as produced state of the FRP-elements. The length of the 7.5 mm diameter bar amounts to 10 mm.

Initial material data

The specimens have to be from the same production lot. Their short-term tensile strength has to be determined before.

Sampling and pre-conditioning of specimen

Samples are cut from coils or rods and are stored 14 days prior to testing at 20 °C/65 % r.h.

7. Cross-section of composite

The cross-section of the FRP-element is defined by 7.5 mm in diameter.

8. Accuracy of testing and measuring devices

The testing machine has to satisfy the conditions given in ISO 5893. The displacement of the transverse heads of the testing machine have to be measured with LVDT. Tests should be performed in a laboratory climate of 20 °C/65 % r.h.

9. Miscellaneous information

10. Test performance

The test will be performed in a conventional servohydraulic testing machine. The specimen (FRP-elements, diameter 7.5 mm, length l = 10 mm) are adjusted and fixed among the transverse heads. The specimen is subjected to a compressive force in a deformation-controlled fashion with a loading speed of 0.0125 mm/s. The force is measured with a load cell and is recorded. The corresponding displacement of the transverse heads of the testing machine is measured with LVDT. The determination of a complete force-displacement diagram should be possible.

11. Evaluation of test results

The measured force corresponds with the inventory interlaminar shear strength between the fibers of the specimen. The interlaminar shear strength is determined by the following relation:

$$f_{\tau ci} = \frac{F_u}{\pi \cdot d \cdot L}$$

Test mean values and the standard deviation of the results have to be calculated. Because of the spread of the results 15 specimen should be tested.

12. Test report

The test report must contain the following information:

- complete identification of the tested material (type, manufacturer, method and date of manufactoring, production lot number etc.)
- Furthermore the test report contains all relevant informations and test data to the items above mentioned.

5.5 Internal Standard for Surface Shear Strength Testing

1. Aim of the test

It is the aim of the test to quantify the force transfer between the fibers and their outer coating.

2. Reference to other standards

3. Short description of the test method

The determination of the surface shear strength is based on a pull-out test of FRP-elements, embedded in a resin mortar. The bond length of the FRP-element amounts to 30 mm in the middle third. The embedded FRP-element is subjected to a pull-out force. The value of this force is recorded.

4. Definition and notations

F	force (in general)
F_u	ultimate force
L	total length of specimen
d	effective diameter of the topping slab
L_B	bond length of the embedded specimen
$f_{\tau cs}$	surface shear strength

5. Units

Force	N, kN
Stress	MPa, N/mm^2

6. Test specimen

Shape and dimension

Shape and dimension of the test specimen correspond to the as produced state of the FRP-elements. The embedded length of the FRP element amounts to 30 mm.

Initial material data

(in analogy to interlaminar shear strength)

Sampling and pre-conditioning of specimen

(in analogy to interlaminar shear strength)

7. Cross-section of composite

(in analogy to interlaminar shear strength)

8. Accuracy of testing and measuring devices

(in analogy to interlaminar shear strength)

9. Miscellaneous information

10. Test performance

Test set-up

An overview of the test set-up is given in Fig. 2.13. The specimen is subjected to a tensile force. The loading rate is about 0.04 mm/s.

Number of specimens

It is necessary to test a serie of 10 specimens.

Force and displacement measurement

The force is measured with a load cell during the test. The corresponding displacement at the unloaded end of the specimen is measured with LVDT.

11. Evaluation of test results

The measured force referred to the surface of the specimen corresponds with the surface shear strength between FRP and bond mortar. The surface shear strength is determined by the following relation:

$$f_{\tau ci} = \frac{F_u}{\pi \cdot d \cdot L_B}$$

12. Test report

(in analogy to interlaminar shear strength)

5.6 Internal Standard for Creep Rupture Testing

1. Aim of test

It is the aim of the test to assess the long-term static tensile strength of FRP tensile elements subjected to a specific environment.

2. Reference to other standards

3. Short description of test method

The specimen is subjected to a constant tensile force in combination with a specific environment. The time under force until fracture of the specimen will be recorded.

4. Definitions and notations

L	total length of specimen
L_c	free length between anchorages
L_e	gage length for measurement of axial strain
L_t	contact length of the specimen with the test environment
F	force (in general)
F_{cl}	long-term force
F_{cli}	long-term force on force level α_i
F_{clm}	mean long-term static breaking force
F_{clk}	characteristic long-term static breaking force
F_{cm}	mean short-term tensile breaking force
F_{cri}	strength retention
t	time
t_u	time until fracture

t_{ui}	time until fracture on force level α_i
α_i	force level (F_{cli}/F_{cm})
ε	strain
ε_u	ultimate strain
ε_{cc}	creep strain
σ	stress (in general)
$\sigma_c(t)$	stress at time t

5. Units

Force	N, kN
Stress	MPa, N/mm^2
Displacement	mm
Strain	$^0/_{oo}$

6. Test specimen

Shape and dimension

Shape and dimension of the test specimen correspond to the as-produced state of the FRP element. The specific FRP tensile element is produced in different shapes, dimensions etc. Representative types for the testing must be chosen.

Total length, test length and gage length

The test length L_c is 1000 mm. The gage length L_e for the measurement of the axial strain is L_e = 200 mm.

Initial material data

Specimens have to be from the same production lot. The knowledge of the short-term tensile strength with statistical evaluations acc. to 5.3 is prerequisite for the creep rupture testing.

Sampling and pre-conditioning of specimens

Samples are cut from coils or rods of the same production lot and are stored for at least 14 days prior to testing at 20 °C/65 % r.h.

7. Cross-section of composite

8. Accuracy of testing and measuring devices

The devices to establish and maintain the specific test environment must be calibrated and must guarantee constancy of conditions. The tests are performed in a laboratory with controlled climate 20 °C/65 % r.h.

9. Miscellaneous information

If needed other data or information shall be gathered.

10. Test performance

Test set-up

The specimen is axially loaded with the tensile force F_{cli}. The test will be performed in a specific test set-up, s. 3.2. The specimen is gripped or anchored in such a way that the original tensile strength of the FRP element is not reduced. Furthermore, the laboratory anchorage should not exhibit significant slip of the FRP element during the time under load and should have an efficiency ratio of about 0.96.

The force F_{cli} must be maintained constant. Suitable and accurate devices have to be used to measure the force in course of time. A readjustment must be possible. Tolerance range: $\Delta F_{cl}(t) \leq 0.02\ F_{cli}$.

Environment chamber

For a specific test environment a complete liquid- and air-tight chamber enclosing of the FRP element along the contact length L_t is necessary. Special devices for the control of temperature $\Delta T \leq \pm 3$ K and for the control of the composition of the test solution must be chosen.

Loading and force levels

The specimen has been pre-conditioned prior to the test at 20 °C/65 % r.h. The specimen is subjected to the initial force F_{cli} at 20 °C/65 % r.h., either in a strain-rate controlled or deformation controlled mode. The force F_{cli} is kept constant until fracture occurs or until termination of

the test. Immediately after loading the specific environment has to be activied.

Test environment

The test environment is chosen in such a way that it corresponds to the real environment of the envisaged application of the FRP element. The following test environments are recommended:

Normal environment
T = 20 °C; 65 % r.h.

Wet environment
water at 20 °C or air 20 °C/99 % r.h. (above water level).

Alkaline environment
aqueous saturated solution of $Ca(OH)_2$ + 0.4 n KOH at 20 °C.

Acidic environment
aqueous solution containing aggressive anions (Cl^-), at 20 °C.

The number of specimens per force level must be chosen in such a way that a statistical evaluation of measured times until fracture t_u is possible. It is recommended to test 8 specimens on force level 0.75 and 0.85 and 5 specimens on force level 0.7 and 0.9.

Force and strain measurement

Force is measured with a load cell during the loading, and the axial strain with LVDT along the measuring length L_t. Measurements in the initial test phase should be performed continuously up to 148 h and later on in suitable time intervals. Test data should be recorded and logged.

11. Evaluation of test results

The fracture time t_{ui} of the specimen under a force level α_i are evaluated with suitable statistical methods to obtain mean and characteristic long-term strength values, $F_{clm}(t)$ and $F_{clk}(t)$.

12. Test report

The test report must contain the following information:

- complete identification of the material (type, manufacturer, method and date of manufactoring, production lot number, etc.)

- tensile strength of the material, obtaining to the same production lot.

5.7 Internal Standard for Fatigue Testing

1. Aim of test

The aim of the test is to determine the mechanical behaviour of FRP-tensile elements subjected to pulsating tensile loading. The effects of damages such as delamination and fiber fracture will be characterized.

2. References to international standards

Up to now there are no standards describing the procedure of fatigue testing of unidirectional FRP-elements for the pre- or post-tensioning. The tests will be performed following the German guidelines for acceptance testing of prestressing steel [54].

3. Short description of test method

The specimens with suitable anchorages will be subjected to a pulsating tensile force. All fatigue tests will be performed under load control mode with a stress ratio in fatigue of approx 0.1. The number of load cycles until failure will be recorded. Unbroken specimens will be subjected to a short term tensile test for determination of their residual tensile strength.

4. Definitions and notations

L	total length of specimen
L_c	free length between anchorages
F	force
σ_m; σ_u; σ_o	middle-, lower- and upper stress under dynamic action
$\Delta\sigma$	stress range
N	number of load cycles

5. Units

Force	N, kN
Stress	MPa, N/mm^2

6. Test specimen

Shape and dimension

Shape and dimension of the test specimen correspond to the as-produced state of the FRP element.

Total length, test length

The test specimen will be 1000 mm in the free length. The total length depends on the chosen anchorage. The length for measurement of deformations will be defined after prelimenary tests.

Initial material data

Specimens for fatigue testing have to belong to the same production lot used for short-term testing. Their main material data must be known.

Sampling and pre-conditiong of specimens

Specimens will cut from coils or rods of the used production lot and will then stored for at least 14 days prior to testing at 20 °C/65 % r.h.

7. Cross-section of composite

8. Accuracy of testing and measuring devices

The devices for testing and measuring will be calibrated following ISO 4965 [55].

9. Miscellaneous information

Various information will be given: slip, kind of failure etc.

10. Test performance

Test set-up

The test set-up for fatigue testing is described in Sec. 4.3.

Test environment

The test will be performed in a laboratory climate. Test in alkaline solution should be carried out to registrate the damage mechanism of this environment to the specimen. The following test environments are planned:

a) Normal environment
   Laboratory climate, air (20 °C; 65 % r.h.).

b) Alkaline environment, saturated solution
   (20 °C; $Ca(OH)_2$ + 0.4n KOH).

Frequency of loading

The frequency will be kept constant during the test series. It is about 5 Hz.

Number of specimens

At least 6 specimens on each stress level are necessary. In accordance to the guideline for prestressing steel stress levels of $0.55 \times f_c$ and $0.9 \times f_c$ are necessary.

Force and strain measurement

The loading will be measured with a load cell. Strain gages and displacement pickups registrade strain and elongation of the test specimen during dynamic loading.

Residual strength test

Unbroken specimen after 2×10^6 load cycles are subjected to a short-term tensile test to determine their residual strength (see sec. 5.3).

10. Evaluation of test results

Test results will be evaluated with suitable statistical methods (e.g. arc-sin $\sqrt{P}$-transformation, 2-parameter Weibull distribution) to determine characteristic fatigue life lines.

11. Test report

The test report must contain the following information:

- complete identification of the material (type, manufacturer, method and date of manufactoring, production lot number).
- report on the mechanical short-term properties of the tested material.

Furthermore the test report must contain all relevant information and test data with respect to 1. to 10..

6. LITERATURE

[1] Rostásy, F.S.: Evaluation of potentials and production technologies of FRP; Technical report Task 1; BREU 1-92.

[2] ASTM Standard D 3039-76,"Standard Test Method for Tensile Properties of Fiber-Resin Composites", American Society for Testing and Materials, Philadelphia, 1982.

[3] DIN 53455 "Prüfung von Kunststoffen - Zugversuch", Normenausschuß Materialprüfung, 1981.

[4] ISO/DIS 527 "Plastics-Determination of tensile properties", International Organization for Standardization, Genf, 1978.

[5] EN 61 "Fiber reinforced plastics, tensile properties", European Committee for Standardization, Brussels, 1977.

[6] Chawla,K.K.: Composite Materials. Science and Engenieering, Springer-Verlag, New York, 1987.

[7] Faoro,M.: Optimierung von Klemmplattenverankerungen für HLV-Stäbe. Universität Stuttgart, Institut für Werkstoffe im Bauwesen, Stuttgart, 1983.

[8] Rehm,G.; Schlottke B.: Übertragbarkeit von Werkstoffkennwerten bei Glasfaser-Harz-Verbundstäben, Universität Stuttgart, Institut für Werkstoffe im Bauwesen, Stuttgart, 1987.

[9] Rehm,G.: Gutachterliche Stellungnahme über die Material- und Verbundeigenschaften von HLV-Elementen im Hinblick auf einen Einsatz als Spannbewehrung, Anlage 1, Stuttgart, 1985.

[10] HBG, R&D Department/AKZO: Vorschlag für Entwurfsgrundlagen und Sicherheitskriterien von Arapree, 1989.

[11] Mijnsbergen, J.: Mechanical properties of Arapree. Part 1: Short-term strength and stiffness. Report 25-87-28, TU Delft, 1989.

[12] Faoro, M.: Zum Tragverhalten kunstharzgebundener Glasfaserstäbe im Bereich von Endverankerungen und Rissen in Beton. Dissertation, Universität Stuttgart, 1988.

[13] Kepp, B.: Prüfung und Optimierung verschiedener Konstruktionselemente für die temporäre und permanente Spannkraftüberleitung aus HLV-Bewehrungssträngen in Beton- und Erdbaukörper über geeignete Verankerungselemente. Untersuchungsbericht Nr. 82649, iBMB/TU Braunschweig, 1982.

[14] Chiao, C.C.; Moore, R.L.; Chiao, T.T.: Measurement of shear properties of fibre composites; Part 1: Evaluation on test methods, Composites, July 1977.

[15] Loveless, H.S.; Ellis, J.H.: A Comparison of Methods for Determining the Shear Properties of Glass/Resin Unidirectional Composites. Journal of Testing and Evaluation, Vol.5, No.5; 1977, pp. 369-374.

[16] ASTM-Standard D 2344 "Standard Test Method for Apparent Interlaminar Shear Strength of Parallel Fiber Composites by Short-Beam-Method", American Society for Testing and Materials, Philadelphia, 1984.

[17] EN 2377 "Prüfverfahren zur Bestimmung der scheinbaren interlaminaren Scherfestigkeit", European Committee for Standardization, Brussels, 1989.

[18] DIN 29971 "Unidirektionalgelege-Prepreg aus Kohlenstoffasern und Epoxidharz", 1991.

[19] Elkink, F.: Short-beam ILSS-metingen aan Arapree (in dutch). Akzo Research Arnheim, 03.09.88.

[20] Schlottke, B.; Franke, L.; Hermann, G.: Interlaminare Schubfestigkeit. Universität Stuttgart, Institut für Werkstoffe im Bauwesen, Stuttgart 1983.

[21] Schlottke, B.; Faoro, M.: Ermittlung der Materialkennwerte von HLV-Elementen unter kurzzeitiger Beanspruchung. Universität Stuttgart, Institut für Werkstoffe im Bauwesen, Stuttgart, 1985.

[22] Faoro, M.: Einflußgrößen auf die experimentelle Ermittlung der Verbundtragfähigkeit der HLV-Elemente im Verankerungsmörtel. Technischer Bericht Nr. Z 5 - 90/2, Strabag Bau-AG, Köln, 1990.

[23] Sippel, T.M.: Stellungnahme und ergänzende Versuche zum Verbundverhalten von HLV-Elementen im Verankerungsmörtel. Bericht Nr. S 2 / 021-90/3 vom 08.01.1991 des Institutes für Werkstoffe im Bauwesen, Universität Stuttgart, 1991.

[24] Faoro, M.: Prüftechnische Fragen und Einflußgrößen auf die Materialkennwerte kunstharzgebundener Glasfaserstäbe. Technischer Bericht Nr. Z 8-91/3, 1991.

[25] Chiao, T.T.; Wells, J.E.; Moore, R.L.; Hamstad, M.A.: Stress-Rupture Behavior of Strands of an Organic Fiber/Epoxy Matrix. 3rd Conf. on Composite Materials: Testing and Design, ASTM STP. 546, 1974, pp. 209-220.

[26] den Uijl, J.A.: Mechanical properties of Arapree. Part 4: Creep and stress-rupture. Report 25-87-31, TU Delft, 1991.

[27] Aveston, J.: Long term strength of glass reinforced plastics in wet environments. Advances in Composite Materials, Proceedings of the Third Conference on Composite Materials, Paris, 26.08.1980.

[28] Christensen, R.M.: Residual-Strength Determination in Polymeric Materials. Journal of Rheology, 25(5), pp. 529-536 (1981).

[29] Chiao, T.T; Chiao, C.C., Sherry, R.J.: Lifestimes of fiber composites under sustained tensile loading. International Conference Fracture Mechanics and Technology, Hong Kong, 1977.

[30] Glaser, R.E.; Christensen, R.M.; Chiao, T.T.: Theoretical Relations Between Static Strength and Lifetime Distribution for Composites: An Evaluation. Composites Technology Review, Band 6, Heft 4, S. 164-167, 1984.

[31] Glaser, R.E.; Moore, R.L.;Chiao, T.T.: Life Estimation of an S-Glass/ Epoxy Composite Under Sustained Tensile Loading. Composites Technology Review, Band 5, Heft 1, S. 21-26, 1983.

[32] Rehm, G.; Franke, L.; Patzak, M.; Zur Frage der Krafteinleitung in kunstharzgebundene Glasfaserstäbe. DAfStb Heft 304, 1979, S.19-43.

[33] Rostásy, F.S.; Budelmann, H.: FRP-Tendons for the post-tensioning of Concrete Structures. ASCE & Spec. Conf.: Advancered Composites Materials in Civil Engineering Structures, Las Vegas, 1991, S. 155-166.

[34] Cook, J.; Howard, A.; Parret, N.J.: Creep and Static fatique of Aromatic Polyamide Fibres. Ministry of Defence, UK, pp. 193-198, 1982.

[35] den Uijl, J.A.: Mechanical properties of Arapree. Part 2: Fatique strength. Report 25-87-29, TU Delft, 1990.

[36] Chiao, T.T; Sherry, R.J.; Hetherington, N.W.: Experimental Verification of an Accelerated Test for Predicting the Lifetime of Organic Fiber Composites, Composite Materials. Band 11, University of California, S. 79-91, 1977.

[37] Phoenix, S.L.; Wu, E.M.: Statistics for the Time-Dependent Failure of Kevlar-49/Epoxy Composites: Micromechanical Modeling and Data Interpretation. Forschungsbericht UCLR-53365, Lawrence Liverpool Laboratory, University of California, 1983.

[38] Weibull, W.: A statistical distribution function of wide applicability. J. Appl. Mech. 18 (1951), No.3, p. 324.

[39] Rosen, W.: Tensile failure of fibrous composites. AIAA Aerospace Sciences Meeting Jan. 20-22(1964), pp. 64-73.

[40] Lifshitz, M.J.; Rotem, A.: Longitudinal tensile failure of unidirectional fibrous composites. J. of Mat. Sci. 7(1972), p. 861.

[41] Franke, L; Overbeck, E.; Meyer, H.-J.: Vorhersage der Zeitstandfestigkeit von GFK-Stäben. Bautechnik 68, 1991, H.1, S. 21-24.

[42] Franke, L.: Schadensakkumulation und Restfestigkeit im Licht der Bruchmechanik. Fortschritte im konstruktiven Ingenieurbau, Rehm-Festschrift, München, 1984, S. 187-197.

[43] Rostásy, F.S.; Kepp, B.: Zum Verhalten dynamisch beanspruchter GFK-Spannglieder. Forschungsbericht, TU Braunschweig, 1986.

[44] Rehm, G.: Gutachterliche Stellungnahme über die Material- und Verbundeigenschaften von HLV-Elementen im Hinblick auf einen Einsatz als Spannbewehrung. Anlage 3, Stuttgart, 1985.

[45] Budelmann, H.; Kepp, B.; Rostásy, F.S.: Fatique behavior of Bond-Anchored Unidirectional Glass-FRP's. ASCE Materials Eng. Congr., Denver, Aug.1990, Vol. 2, pp. 1142-1151.

[46] den Uijl, J.A.: Mechanical properties of Arapree. Part 2: Fatique strength. Report 25-87-29, TU Delft, 1990.

[47] Walton, J.M.; Yeung, Y.T.C.: The fatique Performance of Structural Strands of Pultruded Composite Rods. Journal of the Institute of Mechanical Engineers, London, C286/86, 1986, pp. 315-320.

[48] Jessen, S.M., Plumtree, A.: Fatique damage accumulation in pultruded glass/polyester rods, Composites, Band 20, Heft 6, S. 559 ff., 1989.

[49] Franke, L.; Overbeck, E.: Dauerschwingverhalten von Glasfaserverbundstäben im anwendungsorientietem Zugschwellbereich. Bautechnik 66, 1989, H. 3, S. 90-92.

[50] Franke, L.; Wolff, R. Fibre Glass Tendons for Presstressed Concrete Bridges. IABSE-Congress, Helsinki, June 1988, pp. 51-56.

[51] Smolczyk, H.-G.: Flüssigkeit in den Poren des Betones - Zusammensetzung und Transportvorgänge in der flüssigen Phase des Zementsteines. Beton-Information 1-84, Düsseldorf 1984.

[52] Equilibria of the chemical composition of concrete pore solution Part 1: Comparative study of synthetic and extracted solutions / Part 2: Calculation of the equilibria constants of the synthetic solutions. Cement and Concrete Research, Vol. 17/18, pp. 173-182 / pp. 342-350, 1987/1988.

[53] ISO 5893 "Rubber and plastics test equipment - Tensile, flexural and compression testing machines", Genf, 1985.

[54] Richtlinie für Zulassungs- und Überwachungsprüfungen an Spannstählen, Anlage 1: Bestimmungen für die Durchführung von Dauerschwingversuchen an Spannstählen, IfBt, Berlin , 1977.

[55] ISO 4965 "Axial load fatigue testing machines-Dynamic force calibration-Strain gauge technigue", International Organization for Standartization, Genf, 1979.